Instability of viscoelastic curved liquid jets with surfactants

Alsharif, Abdullah; Uddin, Jamal

DOI:
10.1016/j.jnnfm.2014.12.001

License:
Other (please specify with Rights Statement)

Document Version
Peer reviewed version

Citation for published version (Harvard):
Alsharif, AM & Uddin, J 2015, 'Instability of viscoelastic curved liquid jets with surfactants', Journal of Non-Newtonian Fluid Mechanics, vol. 216, pp. 1-12. https://doi.org/10.1016/j.jnnfm.2014.12.001

Instability of viscoelastic curved liquid jets with surfactants

Abdullah Madhi Alsharif, Jamal Uddin

PII: S0377-0257(14)00218-3
DOI: http://dx.doi.org/10.1016/j.jnnfm.2014.12.001
Reference: JNNFM 3617

To appear in: *Journal of Non-Newtonian Fluid Mechanics*

Received Date: 2 April 2014
Revised Date: 30 October 2014
Accepted Date: 7 December 2014

Please cite this article as: A.M. Alsharif, J. Uddin, Instability of viscoelastic curved liquid jets with surfactants, *Journal of Non-Newtonian Fluid Mechanics* (2014), doi: http://dx.doi.org/10.1016/j.jnnfm.2014.12.001

Instability of Viscoelastic Curved Liquid Jets with Surfactants

Abdullah Madhi Alsharif[a], Jamal Uddin[a,*],

[a]*School of Mathematics, The University of Birmingham. Edgbaston, Birmingham. B15 2TT. UK*

Abstract

The prilling process is a common technique utilised in different applications in many industrial and engineering processes. Typically in such a process a liquid jet emerges from an orifice and thereafter breaks up into small spherical droplets of various sizes due to interfacial instabilities. As is common in many industrial applications the fluid used is often a mixture of various fluids and will typically contain polymers or other additives which will cause the fluid to behave like a non-Newtonian fluid. Furthermore, surfactants may be used in such processes to manipulate the size of the resulting droplets. In this paper, we model the fluid as a viscoelastic liquid and use the Oldroyd-B constitutive equation. We reduce the governing equations into a set of one-dimensional equations by using an asymptotic analysis and then we examine steady state solutions for viscoelastic rotating liquid jets with surfactants. We thereafter examine small perturbations to this steady state to investigate both linear and non-linear instability of the liquid jet.

Keywords:
Viscoelastic jets, break-up, rotation, surfactants

1. Introduction

The fragmentation of viscoelastic liquid jets into droplets has many industrial applications such as sprays, fertilizers, ink jets and roll coating (see Eggers *et al.* [15], Middleman *et al.* [24], Basaran [5] and Mckinley [22] for

*Corresponding Author:
J.Uddin@bham.ac.uk (Jamal Uddin).

reviews of the various applications). The widespread use of devices which utilise a liquid jet at ever decreasing length scales and with a need for greater accuracy motivates the need to understand the mechanisms of the capillary instability and break-up of non-Newtonian liquid jets. Rayleigh [30], who is credited with being the first to examine theoretically the instability of incompressible inviscid liquid jets, identified that liquid jets are unstable to waves which have a wavelength greater than their circumference. Moreover, it was shown that a most unstable wave exists, typically now referred to as the Rayleigh mode, which was responsible for breakup and droplet formation. The presence of viscosity within the fluid was considered by Weber [42], who found that the wavelength of the most unstable mode is increased by viscosity. Since these two pioneering works there has been a wealth of publications examining various features associated with instability of straight liquid jets including variations associated with jet structure, different liquids and linear and nonlinear growth (see Eggers [14]).

However, despite the abundance of literature on straight liquid jets relatively little has been developed in terms of liquid jets that are curved either by the action of some body force such a gravity or an electric field or by the application of a solid body rotation to the container from which the jet emerges. The latter case is particularly relevant to the industrial prilling process where curved jets are produced due to centrifugal instabilities. The work of Wallwork *et al*. [41] was the first to examine such a scenario and in that work the governing equations and linear stability of small disturbances along an inviscid curved liquid jet was considered. The authors also conducted some experiments for inviscid rotating liquid jets to complement their theoretical works and found agreement between the two. Wong *et al*. [44] conducted a series of experiments of viscous liquid jets to see the effect of different parameters on trajectory and droplet formation of the jet. Decent *et al*. [12] extended the analysis to include gravity in the examination of linear stability by Wallwork [40]. Moreover, the influence of viscosity on the trajectory and stability of the break-up of rotating liquid jets has been examined by Decent *et al*. [13]. Non-Newtonian fluids have been investigated by Uddin *et al*. [39] who used the power-law model to examine the linear instability of a rotating liquid. Uddin [38] examined non-linear temporal solutions of the governing equations for a rotating liquid jet by solving numerically, using a finite difference scheme based on the Lax Wendroff method, the governing equations based on the slender jet assumption.

Surfactants, which have a tendency to reduce the surface tension of a free surface, have been used in many free surface flows to alter the dynamics near the locality of breakup or rupture (see Xue *et al*. [45]). A numerical study has been used by Renardy [31] to find the break-up of Newtonian case and viscoelastic liquid jets for the Giesekus model and upper convected Maxwell model. The stability of viscoelastic jets has been discussed by Middleman [24]. Goldin *et al*. [17] compared the linear stability between inviscid, Newtonian and viscoelastic liquid jets. Mageda & Larson [21] used the Oldroyd-B model for ideal elastic liquids (called Boger fluids) for investigating the rheological behavior of polyisobutylene and polystyrene when the shear rates are low. Yildirim and Basaran [50] studied the threads of shear-thinning jets without surfactants and they found that shear-thinning plays an important role in determining the shape of the interface near breakup. They also investigated the break-up dynamics of liquid jets by using the Carrea model and compared the results with one-and two-dimensional models. The beads-on-string structure was studied by Clasen *et al*. [9] using the Oldroyd-B model. Ardekani *et al*. [4] investigated the dynamics of beads-on-string structure and filament thread for weakly viscoelastic jets by using the Giesekus constitutive equation and they compared the results to those of the Oldroyd-B model. Bhat *et al*. [6] examined formation of beads-on-a-string structures and found that there are sub-satellite beads in their experiments. Mckinley and Tripathi [23] and Anna and Mckinley [2] conducted experiments to observe various stages of the capillary break-up of viscoelastic liquid jets. An experimental study has been conducted by Zhang and Basaran [47] to investigate the effects of viscosity and surface tension. The majority of these studies of either Newtonian or non-Newtonian fluids has been examined without surfactants. However, many authors have studied the effects of adding small amounts of surfactants on straight liquid jets. For example, Whitaker [43] examined the instability of inviscid liquid jets with surfactants. The linear instability of viscous liquid jets and a surfactant has been carried out by Hansen *et al*. [18]. They have found that the growth rate decreases with including surfactants. Anshus [3] investigated theoretically the effect of surfactants on liquid jets in two cases which are compressible and incompressible. He found that the surfactants decrease the growth rate, especially in the case of incompressible liquid jets. Craster *et al*. [11] studied Newtonian liquid jets with surfactants by using a one-dimensional model. The case of weakly viscoelastic jets with surfactants has been examined by Zhang *et al*. [48] in a study in which they discussed the influence of the viscos-

ity ratio, using the Oldroyd-B model. Timmermans & Lister [35] have used a nonlinear analysis to study a surfactant laden thread in inviscid liquid jets. They used a one-dimensional nonlinear model to examine the effect of the surfactant on the change of surface tension gradients. Ambravaneswaran & Basaran [1] also used a one-dimensional approximation model to investigate the nonlinear effects of insoluble surfactants on the break-up of stretching liquid bridges. Uddin [38] investigated the effects of surfactants on the instability of rotating liquid jets. He discovered that surfactants reduce the growth rate of liquid curved jets and hight rotation rates enhance the role of surfactants on break-up lengths. Stone & Leal [34] examined the break-up of liquid jets with surfactants by extending the work of Stone *et al*. [32] to include insoluble surfactants. Viscous liquid jets and soluble surfactants have been studied by Milliken *et al*. [25] and Milliken & Leal [26]. They observed that Marangoni stress decreased with increasing the viscosity and surfactant solubility.

In this paper, we will extend the work of Decent *et al*. [13] to investigate the break-up of viscoelastic liquid curved jets with surfactants by using the Oldroyd-B model. Furthermore, we reduce the governing equations into a set of non-dimensional equations to captures the dynamics of the break-up of low viscosity elastic solutions with insoluble surfactants. We also use an asymptotic approach to find steady state solutions and then examine a linear instability analysis on these solutions. In this study, we numerically solve these equations using a finite difference scheme based on the Lax Wendroff method to determine the break-up lengths and main and satellite droplet sizes.

2. Problem Formulation

In this section we develop the governing equations which govern the dynamics of a liquid jet emerging from a rotating orifice with applications to the industrial prilling process. Since the derivation has been explained in length elsewhere (see P$\breve{a}$r$\breve{a}$u *et al*. [28, 29]) we will not motivate the equations in great detail. In this regards, we assume that we have a large cylindrical container which has radius s_0 and rotates with angular velocity Ω. The liquid emerges from an orifice which is made in the side of this container. The radius of the orifice, a, is very small compared with the radius of the container. This problem is examined by choosing a coordinate system (X, Y, Z) rotating with the container, having an origin at the axis of the container. The

position of the orifice is at $(s_0, 0, 0)$. Due to the rotation of the container, the liquid leaves the orifice following a curved trajectory. In this problem, which is the prilling process, we consider that the centripetal acceleration of the jet is very large compared with the force of gravity. Under this assumption one may assume the jet moves in the (X, Z) plane, so that the centerline can be described by coordinates $(X(s,t), 0, Z(s,t))$, where s is the arc-length along the middle of the jet which emerges from the orifice and t is the time (see Wallwork [40]). In any cross-section of the jet we also have plane polar coordinates (n, ϕ), which are the radial and azimuthal direction and have unit vectors which are $\mathbf{e_s}$, $\mathbf{e_n}, \mathbf{e}_\phi$ (see Decent *et al.* [12]). The velocity components for this problem are $(\boldsymbol{u}, \boldsymbol{v}, \boldsymbol{w})$, where $\boldsymbol{u}$ is the tangential velocity, $\boldsymbol{v}$ is the radial velocity and $\boldsymbol{w}$ is the azimuthal velocity.

Initially, we outline the continuity, momentum and constitutive equations of motion. Due to the surfactant concentration, we have a convection-diffusion equation along the liquid interface. We use the Oldroyd-B model for viscoelastic term. These equations therefore take the form

$$\boldsymbol{\nabla} \cdot \boldsymbol{u} = 0,$$

$$\rho\Big(\frac{\partial \boldsymbol{u}}{\partial t} + \boldsymbol{u} \cdot \boldsymbol{\nabla} \boldsymbol{u}\Big) = -\boldsymbol{\nabla} p + \boldsymbol{\nabla} \cdot \boldsymbol{\tau} - 2\,\boldsymbol{w} \times \boldsymbol{u} - \boldsymbol{w} \times (\boldsymbol{w} \times \boldsymbol{r}),$$

$$\boldsymbol{\tau} = \mu_s(\boldsymbol{\nabla} \boldsymbol{u} + (\boldsymbol{\nabla} \boldsymbol{u})^T) + \boldsymbol{T},$$

$$\frac{\partial \boldsymbol{T}}{\partial t} + (\boldsymbol{u} \cdot \boldsymbol{\nabla})\boldsymbol{T} - \boldsymbol{T} \cdot \boldsymbol{\nabla} \boldsymbol{u} \cdot \boldsymbol{T} - (\boldsymbol{\nabla} \boldsymbol{u})^T \cdot \boldsymbol{T} = \frac{1}{\lambda}\Big(\mu_p \boldsymbol{\gamma} - \boldsymbol{T}\Big), \qquad (1)$$

where u is the velocity in the form $\boldsymbol{u} = \boldsymbol{u}e_s + \boldsymbol{v}e_n + \boldsymbol{w}e_\phi$, ρ is the density of the fluid, p is the pressure, the angular velocity of the container is $\boldsymbol{w} = (0, w, 0)$, μ_s is the viscosity of the solvent, $\boldsymbol{T}$ is the extra stress tensor that denotes to the term of viscoelastic, and μ_p is the viscosity of the polymer. The surfactant concentration along the jet is given by (see Stone & Leal [34] and Blyth & Pozrikidis [7])

$$\Gamma_t + \boldsymbol{\nabla}_\mathbf{s} \cdot (\Gamma \boldsymbol{u}_\mathbf{s}) + \Gamma(\boldsymbol{\nabla}_\mathbf{s} \cdot \boldsymbol{n})(\boldsymbol{u} \cdot \boldsymbol{n}) = S(\Gamma, B_s) + \boldsymbol{D}_\mathbf{s} \boldsymbol{\nabla}_\mathbf{s}^\mathbf{2} \Gamma, \qquad (2)$$

where $\boldsymbol{\nabla}_\mathbf{s} = (I - \mathbf{nn}) \cdot \nabla$ is the surface gradient operator, $\boldsymbol{D}_\mathbf{s}$ is the surface diffusivity of surfactant, $\boldsymbol{u}_\mathbf{s} = (I - \mathbf{nn}) \cdot \boldsymbol{u}$ is the surface or tangential velocity, and $\boldsymbol{\nabla}_\mathbf{s} \cdot \mathbf{n} = 2\kappa$ where κ is the mean curvature of the free surface. The

surfactant source term, S, takes absorption from the free surface into account, and acts as a function of surfactant concentration on the surface Γ and the bulk B_s. The third term on the left of (2) relates to the effect of normal forces on dilatation by expansion (see Blyth and Pozrikidis [7]). We consider in this study that the diffusivity of surfactant is small ($\boldsymbol{D_s} = 0$) and the surfactant is insoluble (*i.e.*, $S = 0$). For example, if surfactant with typical diffusivity $10^{-10} - 10^{-9}\ mm^2\, s^{-1}$ (Tricot [36]) were added to the liquid-bridge experiments of Zhang, Padgett & Basaran [49] , so that the Peclet number would be at least $10^3 - 10^4$. This approach has been taken by Timmermans & Lister [35] for investigating the linear stability of a liquid thread with surfactants. Uddin [38] examined linear and nonlinear instability of non-Newtonian liquid curved jets with surfactants by using this approach

$$\Gamma_t + \boldsymbol{u} \cdot \boldsymbol{\nabla}\Gamma - \Gamma \mathbf{n} \cdot ((\mathbf{n} \cdot \boldsymbol{\nabla})\boldsymbol{u}) = 0. \tag{3}$$

The boundary conditions are

$$\frac{\partial R}{\partial t} + \mathbf{u} \cdot \nabla R = 0, \tag{4}$$

normal and tangential conditions are

$$p + \mathbf{n} \cdot \mathbf{P} \cdot \mathbf{n} = \sigma \nabla \cdot \mathbf{n}, \tag{5}$$

and

$$\mathbf{t_i} \cdot \mathbf{P} \cdot \mathbf{n} = \mathbf{t_i} \cdot \nabla \sigma, \tag{6}$$

where

$$\mathbf{P} = -p\mathbf{I} + \mu\Big(\nabla \mathbf{u} + (\nabla \mathbf{u})^T\Big) + T,$$

the normal vector is

$$\mathbf{n} = \frac{1}{E}\left(-\frac{\partial R}{\partial s}\frac{1}{h_s}\mathbf{e_s} + \mathbf{e_n} - \frac{\partial R}{\partial \phi}\frac{1}{R}\mathbf{e}_\phi\right), \tag{7}$$

tangential vectors are

$$\mathbf{t_1} = \mathbf{e_s} + \frac{1}{h_s}\frac{\partial R}{\partial s}\mathbf{e_n} \text{ and } \mathbf{t_2} = \frac{1}{R}\frac{\partial R}{\partial \phi}\mathbf{e_n} + \mathbf{e}_\phi,$$

and the arc-length condition is

$$X_s^2 + Z_s^2 = 1. \tag{8}$$

Moreover, there is an another equation, which is the Szyskowski equation that is given by

$$\sigma = \tilde{\sigma} + \Gamma_\infty R_g T \log\Big[\frac{\Gamma_\infty - \Gamma}{\Gamma_\infty}\Big], \tag{9}$$

which is a special case from the Frumkin equation of state $\sigma = \tilde{\sigma}+\Gamma_\infty R_g T(\log(1-\frac{\Gamma_\infty}{\Gamma})+\frac{A\Gamma_\infty^2}{2\Gamma^2})$, where $\tilde{\sigma}$ is the surface tension of the liquid in the absence ($\Gamma = 0$) of any surfactant, Γ_∞ is the maximum packing concentration of surfactant, R_g is the universal gas constant, T is the temperature, A is the molecular interaction parameter and Γ is the critical micelles concentration (CMC). This equation gives the relation between the surfactant concentration Γ and the surface tension of the liquid-gas interface. We can express our equations in dimensionless terms by using the following transformations

$$\begin{aligned}
&\bar{u} = \frac{u}{U}\ , \quad \bar{v} = \frac{v}{U}, \quad \bar{w} = \frac{w}{U}, \quad \bar{n} = \frac{n}{a}, \quad \epsilon = \frac{a}{s_0},\\
&\bar{R} = \frac{R}{a}, \quad \bar{T} = \frac{s_0}{U\mu_0}T, \quad \bar{s} = \frac{s}{s_0}, \quad \bar{t} = \frac{U}{s_0}\,t, \quad \bar{p} = \frac{p}{\rho U^2},\\
&\bar{X} = \frac{X}{s_0}, \quad \bar{Z} = \frac{Z}{s_0}, \quad \bar{\sigma} = \frac{\sigma}{\tilde{\sigma}}, \quad \bar{\Gamma} = \frac{\Gamma}{\Gamma_\infty},
\end{aligned} \tag{10}$$

where u, v and w are the tangential, radial and azimuthal velocity components, U is the exit speed of the jet in the rotating frame, s_0 is the radius of the cylindrical drum, a is radius of the orifice, ϵ is the aspect ratio of the jet, T is the extra stress tensor, μ_0 is the total viscosity of the solvent and the polymer and σ and Γ are dimensionless with respect to the surface tension and the surfactant concentration, then dropping over bars. The equation of motion is the same which is found in P$\breve{a}r\breve{a}$u *et al.* [29], but there are extra terms related to viscoelastic terms as follows

$$\epsilon n\frac{\partial u}{\partial s} + h_s\left(v + n\frac{\partial v}{\partial n} + \frac{\partial w}{\partial \phi}\right) + \epsilon n\left(v\cos\phi - w\sin\phi\right)\left(X_s Z_{ss} - Z_s X_{ss}\right) = 0, \tag{11}$$

$$\begin{aligned}
&(N.S)_{(s)} + \frac{1}{h_s\, Re}\Bigg[\epsilon\frac{\partial T_{ss}}{\partial s} + 2\epsilon(v\cos\phi - w\sin\phi)(X_s Z_{ss} - Z_s X_{ss})T_{ss} +\\
&\frac{\partial T_{sn}}{\partial n}h_s + \frac{h_s}{n}\frac{\partial T_{s\phi}}{\partial \phi} + \frac{h_s v}{n}\,T_{s\phi}\Bigg],
\end{aligned} \tag{12}$$

$$(N.S)_{(n)} + \frac{1}{h_s Re}\Bigg[\epsilon\frac{\partial T_{sn}}{\partial s} + \epsilon(v\cos\phi - w\sin\phi)(X_s Z_{ss} - X_{ss} Z_s)\, T_{sn} -$$

$$\epsilon u\cos\phi T_{sn} + \frac{\partial T_{nn}}{\partial n}h_s + \frac{h_s}{n}\frac{\partial T_{n\phi}}{\partial \phi} + \frac{h_s v}{n}\, T_{n\phi} - \frac{w}{n}h_s T_{n\phi}\Bigg], \tag{13}$$

$$(N.S)_{(\phi)} + \frac{1}{h_s\, Re}\Bigg[\epsilon\frac{\partial T_{s\phi}}{\partial s} + \epsilon(v\cos\phi - w\sin\phi)(X_s Z_{ss} - X_{ss} Z_s)\, T_{s\phi} -$$

$$\frac{\epsilon u}{h_s}T_{s\phi}\sin\phi(X_s Z_{ss} - X_{ss} Z_s) + \frac{\partial T_{n\phi}}{\partial n}h_s + \frac{h_s}{n}\frac{\partial T_{\phi\phi}}{\partial \phi} + \frac{2h_s v}{n}\, T_{\phi\phi}\Bigg], \tag{14}$$

where $(N.S)_{(s)}$, $(N.S)_{(n)}$ and $(N.S)_{(\phi)}$ are the Navier-Stokes equations in the axial, radial and azimuthal direction respectively as found in Păraău *et al.* [29] in which $\frac{Re}{\alpha_s} = Re$, the dimensionless parameters here are the Rossby number $Rb = \frac{U}{s_0\Omega}$, the Weber number $We = \frac{\rho U^2 a}{\sigma}$, the Reynolds number $Re = \frac{\rho U a}{\mu_0}$, the Deborah number $De = \frac{\lambda U}{s_0}$ and the ratio between the viscosity of the solvent and the total of the viscosity is $\alpha_s = \frac{\mu_s}{\mu_0} = \frac{\mu_s}{\mu_s+\mu_p}$. Using typical parameter values encountered in prilling (see Wong *et al.* [44]) of $U \sim 0.3 - 1$ ms^{-1} and $s_0 \sim 0.04$ m and typical relaxation times of elastic fluids $\lambda \sim 10^{-3} - 10$ (see Entov & Hinch [16]) we can estimate the range of Deborah number values as $De \sim 250 - 0.008$. The equations of the extra stress tensor are in the appendix. The surfactant concentration equation is (see Uddin [38])

$$\begin{aligned}\Gamma_t \;=\; & -\frac{u}{h_s}\frac{\partial \Gamma}{\partial s} - \frac{v}{\epsilon}\frac{\partial \Gamma}{\partial n} - \frac{w}{\epsilon n}\frac{\partial \Gamma}{\partial \phi} + \\ & \frac{\Gamma}{E}\Big(\frac{\epsilon^2}{h_s^2}\Big(\frac{\partial R}{\partial s}\Big)^2\frac{\partial u}{\partial s} - \frac{1}{h_s}\Big(\frac{\partial R}{\partial s}\Big)\frac{\partial u}{\partial n} + \frac{1}{nRh_s}\frac{\partial R}{\partial \phi}\frac{\partial R}{\partial s}\frac{\partial u}{\partial \phi} - \frac{\epsilon}{h_s^2}\Big(\frac{\partial R}{\partial s}\Big)\frac{\partial v}{\partial s} + \\ & \frac{1}{\epsilon}\frac{\partial v}{\partial n} - \frac{1}{\epsilon nR}\frac{\partial R}{\partial \phi}\frac{\partial v}{\partial \phi} + \frac{\epsilon}{Rh_s^2}\frac{\partial R}{\partial \phi}\frac{\partial R}{\partial s}\frac{\partial w}{\partial s} - \frac{1}{R}\frac{\partial R}{\partial \phi}\frac{\partial w}{\partial n} + \frac{1}{\epsilon nR^2}\Big(\frac{\partial R}{\partial \phi}\Big)^2\frac{\partial w}{\partial \phi}\Big).\end{aligned} \tag{15}$$

3. The Non-dimensionalisation of Boundary Conditions

It can be found that the normal stress condition is

$$p - \frac{2\alpha_s}{Re}\frac{1}{E^2}\Bigg(\epsilon^2\left(\frac{\partial R}{\partial s}\right)^2\frac{1}{h_s^3}\left(\frac{\partial u}{\partial s} + (v\,cos\phi - \sin\phi)(X_s Z_{ss} - Z_s X_{ss}) + \frac{h_s}{2\alpha_s}T_{ss}\right)$$

$$+\frac{1}{\epsilon}\frac{\partial v}{\partial n}+\frac{1}{2\alpha_s}T_{nn}+\frac{1}{\epsilon\,R^3}\left(\frac{\partial R}{\partial\phi}\right)^2\left(\frac{\partial w}{\partial\phi}+v+RT_{\phi\phi}\right)-$$
$$\frac{\epsilon}{h_s}\frac{\partial R}{\partial s}\left(\frac{1}{h_s}\frac{\partial v}{\partial s}+\frac{1}{\epsilon}\frac{\partial u}{\partial n}-\frac{u}{h_s}\,cos\phi(X_sZ_{ss}-Z_sX_{ss})+\frac{1}{2\alpha_s}T_{sn}\right)+$$
$$\frac{\epsilon}{Rh_s}\frac{\partial R}{\partial s}\frac{\partial R}{\partial\phi}\left(\frac{1}{\epsilon\,R}\frac{\partial u}{\partial\phi}+\frac{u}{h_s}\,\sin\phi(X_sZ_{ss}-Z_sX_{ss})+\frac{1}{h_s}\frac{\partial u}{\partial s}+\frac{1}{2\alpha_s}T_{s\phi_s}\right)$$
$$-\frac{1}{R}\frac{\partial R}{\partial\phi}(R\frac{\epsilon\partial w}{\partial n}-\frac{\epsilon w}{R}+\frac{\epsilon}{R}\frac{\partial v}{\partial\phi}\Big)=\frac{\sigma\,\kappa}{We}\ \text{on}\ n=R(s,t), \tag{16}$$

where

$$\kappa=\frac{1}{h_s}\left(-\epsilon^2\frac{\partial}{\partial s}\left(\frac{n}{Eh_s}\frac{\partial R}{\partial s}\right)+\frac{\partial}{\partial n}\left(\frac{nh_s}{E}\right)-\frac{\partial}{\partial\phi}\left(\frac{h_s}{En}\frac{\partial R}{\partial\phi}\right)\right).$$

$$E=\left(1+\frac{\epsilon^2}{h_s^2}\left(\frac{\partial R}{\partial s}\right)^2+\frac{1}{R^2}\left(\frac{\partial R}{\partial\phi}\right)^2\right)^{\frac{1}{2}}.$$

$$h_s=1+\epsilon n\cos\phi(X_sZ_{ss}-X_{ss}Z_s).$$

The first tangential stress condition is

$$\left(1-\epsilon^2\left(\frac{\partial R}{\partial s}\right)^2\frac{1}{h_s^2}\right)\left\{\epsilon\frac{\partial v}{\partial s}+\,h_s\frac{\partial u}{\partial n}-\epsilon u\cos\phi(Z_sZ_{ss}-X_{ss}Z_s)+\frac{\epsilon}{\alpha_s}T_{sn}\right\}+2\epsilon\frac{\partial R}{\partial s}$$
$$\left\{\frac{\partial v}{\partial n}-\epsilon\frac{\partial u}{\partial s}\frac{1}{h_s}-\frac{\epsilon}{h_s}v\cos\phi-w\sin\phi(X_sZ_{ss}-X_{ss}Z_s)-\frac{\epsilon}{2\alpha_s}\left(T_{ss}-T_{nn}\right)\right\}=$$
$$\frac{\epsilon Re}{We}\Big(\frac{\epsilon}{h_s}\frac{\partial\sigma}{\partial s}+\frac{1}{h_s}\frac{\partial R}{\partial s}\frac{\partial\sigma}{\partial n}\Big), \tag{17}$$

and the second tangential stress condition is

$$\left(1-(\frac{\partial R}{\partial\phi})^2\frac{1}{R^2}\right)\left(\frac{\partial w}{\partial n}-\frac{w}{R}+\frac{1}{R}\frac{\partial v}{\partial\phi}+\frac{\epsilon}{\alpha_s}T_{n\phi}\right)+$$
$$\frac{2}{R}\frac{\partial R}{\partial\phi}\left(\frac{\partial v}{\partial n}-\frac{1}{R}(\frac{\partial w}{\partial\phi}+v)+\frac{\epsilon}{\alpha_s}\left(T_{nn}-T_{\phi\phi}\right)\right)=\frac{\epsilon Re}{We}\Big(\frac{1}{R}\frac{\partial R}{\partial\phi}+\frac{1}{n}\frac{\partial\sigma}{\partial\phi}\Big). \tag{18}$$

Another boundary condition is the arc-length condition $X_s^2 + Z_s^2 = 1$ and also the kinematic condition is

$$h_s \left(\epsilon \frac{\partial R}{\partial t} + (\cos\phi + \frac{1}{n} \frac{\partial R}{\partial t} \sin\phi (X_t Z_s - X_s Z_t) - v + \frac{\partial R}{\partial \phi} \frac{w}{n} \right)$$
$$+ \epsilon u \frac{\partial R}{\partial s} - \epsilon \frac{\partial R}{\partial s} (X_t Z_s - X_s Z_t + \epsilon n \cos\phi (X_s Z_{ss} - Z_s X_{ss})) = 0. \quad (19)$$

4. Asymptotic Analysis

We will consider that u, v, w and p in Taylor's series are expanded in ϵn (see Eggers [14] and Hohman *et al.* [19]) and $R, X, Z, T_{ss}, T_{nn}, T_{\phi\phi}$ in asymptotic series in ϵ. We suppose that the leading order of the axial component of the velocity is independent on ϕ. It is also assumed that small perturbations do not affect the centerline. Therefore, we have

$$[u, v, w, p] = [u_0(s,t), 0, 0, 0] + (\epsilon n)[u_1(s,\phi,t), v_1(s,\phi,t), w_1(s,\phi,t), p_1(s,\phi,t)] + O(\epsilon^2) \quad (20)$$

$$[R, X, Z, T_{ss}, T_{nn}, T_{ij}] = [R_0(s,t), X_0(s,t), Z_0(s,t), T^0_{ss}(s,t), T^0_{nn}(s,t), \epsilon T^0_{ij}(s,t)] +$$
$$(\epsilon)[R_1(s,t), X_1(s,t), Z_1(s,t), T^1_{ss}(s,t), T^1_{nn}(s,t), \epsilon T^1_{ii}(s,t)] + \cdots, \quad (21)$$

where the subscript $\{ij\}$ covers the remaining components. The following expansions have been used for the surfactant concentration Γ and the surface tension σ as

$$[\Gamma, \sigma] = [\Gamma_0(s), \sigma_0(s)+] + \epsilon[\Gamma_1(s), \sigma_1(s)] + O(\epsilon^2), \quad (22)$$

Substitution of the above expansions into the governing equations and collecting terms of similar order yields a set of equations which is tedious and for that reason we do not repeat it here. Instead we simply sate that the resulting analysis will result in the following set of equations

$$(X_s Z_{ss} - X_{ss} Z_s) \left(u_0^2 - \frac{3\alpha_s}{Re} u_{0s} - \frac{\sigma}{We R_0} \right) - \frac{2}{Rb} u_0 + \frac{(X+1)Z_s - Z X_s}{Rb^2} = 0, \quad (23)$$

$$u_{0t} + u_0 u_{0s} = -\frac{1}{We} \frac{\partial}{\partial s} \left(\frac{\sigma_0}{R_0} \right) + \frac{(X+1)X_s + Z Z_s}{Rb^2}$$
$$+ \frac{3\alpha_s}{Re} \left(u_{0ss} + 2u_{0s} \frac{R_{0s}}{R} \right) + \frac{1}{Re} \left(\frac{1}{R_0^2} \frac{\partial}{\partial s} R_0^2 (T^0_{ss} - T^0_{nn}) \right) + \frac{2\sigma_{0s}}{We\, R_0}, \quad (24)$$

along with

$$R_{0t} + \frac{u_{0s}}{2} R_0 + u_0 R_{0s} = 0. \tag{25}$$

These equations are similar to those found in Părău *et al.* [29] except there now appears a few extra terms due to the extra stress tensor. From the extra stress tensor, which is $T_{ss}, T_{sn}, T_{s\phi}, T_{nn}, T_{n\phi}, T_{\phi\phi}$,we have at leading order as follows

$$\frac{\partial T^0_{ss}}{\partial t} + u_0 \frac{\partial T^0_{ss}}{\partial s} - 2 \frac{\partial u_0}{\partial s} T^0_{ss} = \frac{1}{De} \left(2(1-\alpha_s) \frac{\partial u_0}{\partial s} - T^0_{ss} \right), \tag{26}$$

$$\frac{\partial T^0_{nn}}{\partial t} + u_0 \frac{\partial T^0_{nn}}{\partial s} + \frac{\partial u_0}{\partial s} T^0_{nn} = \frac{-1}{De} \left((1-\alpha_s) \frac{\partial u_0}{\partial s} + T^0_{nn} \right). \tag{27}$$

We have the arc-length at order ϵ

$$X_s^2 + Z_s^2 = 1. \tag{28}$$

The last equation which is the surfactant transport equation at leading order is

$$\Gamma_{0t} + u_0 \Gamma_{0s} + \frac{u_{0s}}{2} \Gamma_0 = 0. \tag{29}$$

There is another equation related to the surfactant concentration Γ to the surface tension of the liquid-gas interface, which is Szyskowski equation

$$\sigma = 1 + \beta log(1 - \Gamma), \tag{30}$$

where the parameter $\beta = \Gamma_\infty R_g T/\tilde{\sigma}$ is a measure of the effectiveness of surfactants. In general the centreline of the jet is unsteady however Părău *et al.* [29] has examined the resulting terms produced in the set of equations above when an unsteady centreline is assumed which in turn leads to terms involving $E = Z_s X_t - Z_t X_s$. In the analysis of Părău *et al.* [29] the difference between and steady and unsteady centreline had a maximum deviation of order 10^{-2} of the perturbation of the steady state centerline. Since this value is very small compared to the $O(1)$ values of $X_0(s)$ and $Z_0(s)$ we may therefore use $E \approx 0$ which is a very accurate assumption to be taken from the orifice to the break-up point. Experimentally Wong *et al.* [44] have observed that the centerline of the jet, to leading order, is steady, which means $X_{st} \approx 0$, $Z_{st} \approx 0$ and $E \approx 0$.

5. Steady State Solutions

In this section we search for steady state solutions of the set of equations obtained in the previous section. In total we have six equations in the six variables which are u_0, R_0, X, Z, T^0_{ss} and T^0_{nn} and making use of (25) and (29), we can find $R_0^2 u_0$ and $\Gamma_0^2 u_0$ are constants. Now, we use the initial conditions $R(0) = 1 = u(0)$ and $\Gamma_0(0) = \zeta$, where ζ is the initial surfactant concentration ($0 \leq \zeta \leq 1$), we therefore obtain $R^2 u = 1$ and $\Gamma_0^2 u_0 = \zeta^2$. We then have

$$u_0 u_{0s} = -\frac{(1+\beta log(1-\zeta u_0^{\frac{-1}{2}}))}{We}\frac{u_{0s}}{2\sqrt{u_0}} + \frac{\beta\zeta}{2u_0 We}\frac{u_{os}}{(1-\zeta u_0^{\frac{-1}{2}})} + \frac{(X+1)X_s + ZZ_s}{Rb^2}$$
$$+\frac{3\alpha_s}{Re}\left(u_{0ss} - \frac{u_{0s}^2}{u_0}\right) + \frac{1}{Re}\Big(\frac{\partial}{\partial s}(T^0_{ss} - T^0_{nn}) - \frac{u_{0s}}{u_0}(T^0_{ss} - T^0_{nn})\Big), \tag{31}$$

$$u_0 \frac{\partial T^0_{ss}}{\partial s} - 2\frac{\partial u_0}{\partial s} T^0_{ss} = \frac{1}{De}\left(2(1-\alpha_s)\frac{\partial u_0}{\partial s} - T^0_{ss}\right), \tag{32}$$

$$u_0 \frac{\partial T^0_{nn}}{\partial s} + \frac{\partial u_0}{\partial s} T^0_{nn} = \frac{-1}{De}\left((1-\alpha_s)\frac{\partial u_0}{\partial s} + T^0_{nn}\right), \tag{33}$$

$$(X_s Z_{ss} - X_{ss} Z_s)\left(u_0^2 - \frac{3\alpha_s}{Re} u_{0s} - \frac{1}{We}\Big(1+\beta log(1-\zeta u_0^{\frac{-1}{2}})\Big)\sqrt{u_0}\right) -$$
$$\frac{2}{Rb} u_0 + \frac{(X+1)Z_s - ZX_s}{Rb^2} = 0, \tag{34}$$

and

$$X_s^2 + Z_s^2 = 1. \tag{35}$$

From the equations (31)-(35), we have five unknowns which are X, Z, u_0, T^0_{ss} and T^0_{nn}. This system of non-linear differential equations, which is stiff due to the presence of the viscous term, can be solved by using an implicit finite difference scheme as done by Pătău *et al.* [28, 29] who solved the resulting set of equations using the Newtonian methods. However, the same authors were able to show that the presence of the viscous term did not significantly affect the steady state obtained in the inviscid limit which then resulted in a

simple set of ordinary differential equations. We show, formally, below that the viscous term does not contribute to leading order steady state solutions and we henceforth will solve the above set of equations in the limit $Re \to \infty$. In order to show that the centerline is independent of viscosity to leading order, let us consider the expansions of the form

$$u = u_0(s) + \epsilon u_1(s,n,\phi) + O(\epsilon^2),\ v = v_0(s) + \epsilon v_1(s,n,\phi) + O(\epsilon^2),$$
$$T_{ss} = T^0_{ss}(s) + \epsilon T^1_{ss}(s,n,\phi) + O(\epsilon^2),\ T_{nn} = T^0_{nn}(s) + \epsilon T^1_{nn}(s,n,\phi) + O(\epsilon^2),$$
$$R = R_0(s) + \epsilon R_1(s,n,\phi) + O(\epsilon^2),\ p = p_0(s) + \epsilon p_1(s,n,\phi) + O(\epsilon^2),$$
$$\sigma = \sigma_0(s) + \epsilon \sigma_1(s,n,\phi) + O(\epsilon^2),\ \Gamma = \Gamma_0(s) + \epsilon \Gamma_1(s,n,\phi) + O(\epsilon^2),$$

and set $w = 0$ which means there is no azimuthal velocity. We substitute these into the the governing equation, and therefore obtain at leading order

$$v_1 = -\frac{n}{2}\frac{du_0}{ds}, \tag{36}$$

$$\frac{\partial u_0}{\partial t} + u_0\frac{\partial u_0}{\partial s} = -\frac{\partial p_0}{\partial s} + \frac{1}{Rb^2}\Big((X+1)X_s + ZZ_s\Big) + \frac{\alpha_s Oh}{\sqrt{We}}\Big(\frac{1}{n}\frac{\partial u_1}{\partial n} + \frac{\partial^2 u_1}{\partial n^2} + \frac{1}{n^2}\frac{\partial^2 u_1}{\partial \phi^2}\Big) + \frac{Oh}{\sqrt{We}}\Big(\frac{\partial T^0_{ss}}{\partial s}\Big), \tag{37}$$

$$\frac{\partial p_0}{\partial n} = 0 \text{ and } \frac{\partial p_0}{\partial \phi} = 0,$$

$$u_0\,\frac{\partial T^0_{ss}}{\partial s} - 2\,\frac{\partial u_0}{\partial s}\,T^0_{ss} \;=\; \frac{1}{De}\,\left(2(1-\alpha_s)\,\frac{\partial u_0}{\partial s} \;-\; T^0_{ss}\right), \tag{38}$$

$$u_0\frac{\partial T^0_{nn}}{\partial s} \;+\; \frac{\partial u_0}{\partial s}\,T^0_{nn} \;=\; \frac{-1}{De}\,\left((1-\alpha_s)\frac{\partial u_0}{\partial s} \;+\; T^0_{nn}\right), \tag{39}$$

$$-\cos\phi(X_sZ_{ss} - X_{ss}Z_s)u_0^2 = -\frac{\partial p_1}{\partial n} - \frac{2u_0\cos\phi}{Rb} + \frac{\cos\phi}{Rb^2}\Big((X+1)Z_s - ZX_s\Big), \tag{40}$$

$$\sin\phi(X_sZ_{ss} - X_{ss}Z_s)u_0^2 = -\frac{\partial p_1}{\partial n} - \frac{2u_0\sin\phi}{Rb} - \frac{\sin\phi}{Rb^2}\Big((X+1)Z_s - ZX_s\Big), \tag{41}$$

$$u_0\frac{\partial R_0}{\partial s} = v_1 \text{ on } n = R_0$$

$$p_1 - \frac{2Oh}{\sqrt{We}}\frac{\partial v1}{\partial n} = \frac{\sigma_0}{We}\Big(- \frac{1}{R_0^2}\Big(R_1 + \frac{\partial^2 R_1}{\partial \phi^2}\Big) + \cos\phi(X_s Z_{ss} - X_{ss} Z_s)\Big) \text{ on } n = R_0 (42)$$

and

$$\frac{\partial u_1}{\partial n} = u_0 \cos\phi(X_s Z_{ss} - X_{ss} Z_s) + \frac{Oh^{-1}}{We^{\frac{1}{2}}}\frac{\partial \sigma_0}{\partial s}. \tag{43}$$

We have

$$u_0\frac{\partial u_0}{\partial s} + \frac{\partial p_0}{\partial s} - \frac{(X+1)X_s + ZZ_s}{Rb^2} = \frac{\alpha_s Oh}{\sqrt{We}}\Big(\nabla^2_{n,\phi} u_1\Big) + \frac{Oh}{\sqrt{We}}\frac{\partial T_{ss}}{\partial s}, \tag{44}$$

where

$$\nabla^2_{n,\phi} = \frac{1}{n}\frac{\partial}{\partial n} + \frac{\partial^2}{\partial n^2} + \frac{1}{n^2}\frac{\partial^2}{\partial \phi^2}.$$

Suppose that

$$f(s) = \frac{\sqrt{(We)}}{\alpha_s Oh}\Big(u_0\frac{\partial u_0}{\partial s} + \frac{\partial p_0}{\partial s} - ((X+1)X_s + ZZ_{ss})/Rb^2)\Big) - \frac{1}{\alpha_s}\frac{\partial T^0_{ss}}{\partial s},$$

so that $f(s) = \nabla^2_{n,\phi} u_1$, which is a Neumann problem on a circular domain, where s is a parameter. We determine the solvability condition by multiplying the above equation by $\hat{u}(s, n, \phi)$ and integer over the domain S $(0 \le n \le R_0,\, 0 \le \phi \le 2\pi)$ then we have

$$\int\int_S \Big(\hat{u}\nabla^2_{n\phi} u_1\Big)\, dS = \int\int_S \hat{u} f(s)\, dS,$$

where $\hat{u}$ satisfies the homogeneous Neumann problem such that

$$\nabla^2_{n\phi} u = 0 \text{ with } \frac{\partial \hat{u}}{\partial n} = 0 \text{ on } n = R_0.$$

Greens identity gives

$$\int\int_S \Big(\hat{u}\nabla^2_{n\phi} u_1\Big)\, dS = \int\int_S \hat{u}\frac{\partial u_1}{\partial n}\, d\Omega_S,$$

where Ω_S is the boundary of S. Then we get

$$\int_0^{2\pi}\int_0^{R_0} \hat{u} n f(s) dn d\phi = \int_0^{2\pi}\Big[u\frac{\partial u_1}{\partial n}\Big]_{n=R_0} R_0 d\phi$$

$$= \int_0^{2\pi} [\hat{u}]_{n=R_0} \Big(u_0 \cos\phi (X_s Z_{ss} - X_{ss} Z_s) + \frac{Oh^{-1}}{\sqrt{We}} \frac{\partial \sigma_0}{\partial s} \Big) R_0 d\phi$$

$$= \int_0^{2\phi} [\hat{u}]_{n=R_0} (g(s)\cos\phi + h(s)) R_0 d\phi, \tag{45}$$

where $g(s) = u_0(X_s Z_{ss} - X_{ss} Z_s)$ and $h(s) = \frac{Oh^{-1}}{\sqrt{We}} \frac{\partial \sigma_0}{\partial s}$. The general solution to the homogeneous Neumann problem which is bounded in $0 \leq n \leq R_0$ and is periodic in ϕ with period 2π is $\hat{u} = \gamma(s)$. which means that this result cannot be a function of the radial or azimuthal direction. Then we have

$$\gamma(s) R_0 g(s) [\sin\phi]_0^{2\pi} + \gamma(s) R_0 h(s) [\phi]_0^{2\pi} = \gamma(s) f(s) [\frac{n^2}{2}]_0^{R_0} [\phi]_0^{2\pi}$$

where $R_0 \neq 0$, we thus have $f(s) = \frac{2h(s)}{R_0}$ so that

$$f(s) = \frac{1}{Oh\sqrt{We}} \frac{2}{R_0} \frac{\partial \sigma_0}{\partial s}.$$

Then we have

$$\frac{\partial u_0}{\partial t} + u_0 \frac{\partial u_0}{\partial s} - \frac{(X+1)X_s + Z Z_s}{Rb^2} = -\frac{\partial p_0}{\partial s} + \frac{2}{R_0 We} \frac{\partial \sigma_0}{\partial s}. \tag{46}$$

To obtain p_1, we solve the equations (40),(41) and (42),

$$p_1 = \frac{\sigma_0 n}{R_0 We} \cos\phi (X_s Z_{ss} - X_{ss} Z_s) - \frac{Oh}{\sqrt{We}} \frac{\partial u_0}{\partial s} + h_1(s), \tag{47}$$

where $h_1(s)$ is an arbitrary function of s. We can see that there is no viscous terms in the equation (46), which means that we obtain the same leading order equations for the trajectory in the inviscid case.

We solve this system of nonlinear PDEs as we have mentioned earlier by using the Runge-Kutta method with the boundary conditions at the nozzle are $X(0) = Z(0) = Z_s(0) = T^0_{ss}(0) = T^0_{nn}(0) = 0$ and $u(0) = X_s(0) = 1$. In Figs. 5.1-5.5, we find the jet trajectory, the extra stress tensor (T^0_{ss}, T^0_{nn}) and the jet radius for different values of Rossby and Weber numbers.

In Fig. 1, we show the effects of different values of the initial surfactant concentration ζ on trajectories of the liquid jet. From this figure, it can be

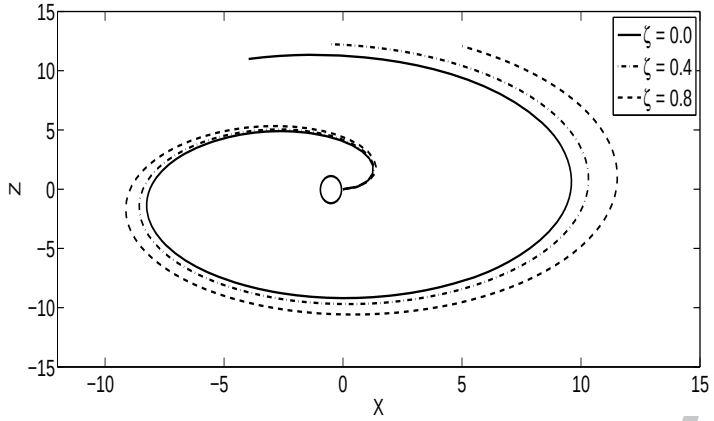

Figure 1: The trajectory of rotating liquid jets with the effect of surfactants, which is solved by using the Runge-Kutta method and emerging from an orifice placed at (0,0). The jet curves increase when the initial surfactant concentration increases. The parameters here are $We = 8$, $Rb = 2$, $De = 20$, $\alpha_s = 0.2$ and $\beta = 0.4$.

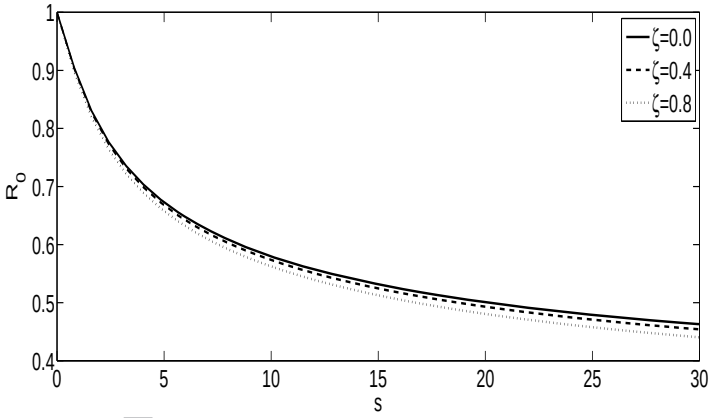

Figure 2: The radius of rotating liquid jets with changing the initial surfactant concentration versus the arc-length s. Here we have $We = 8$, $Rb = 2$, $De = 20$, $\alpha_s = 0.2$ and $\beta = 0.4$. It can be seen that increasing the initial surfactant concentration increases the radius of the jet along the jet.

observed that when ζ is increased, which corresponds to an increase in the initial surfactant concentration, the liquid jets coil less progressively. We also the influence of increasing the initial surfactant concentration ζ on the radius of the jet against arc-length s in Fig. 2. We observe that greater values of

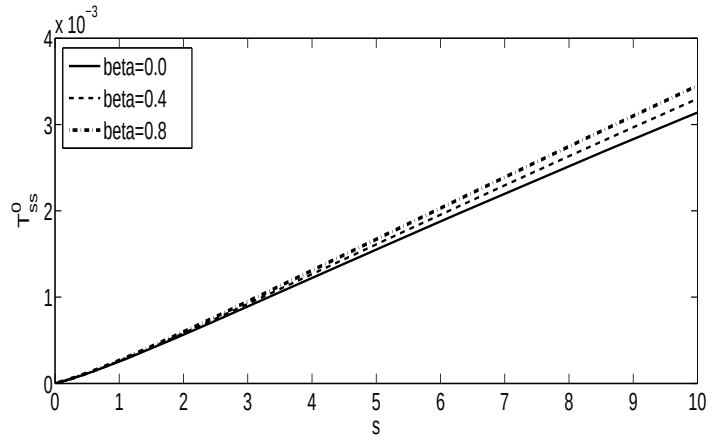

Figure 3: The effect of changing the parameter β of a rotating liquid jet on the extra stress tensor T^0_{ss} along the jet.Here we use $We = 8$, $De = 20$, $\beta = 0.4$, $\alpha_s = 0.2$ and $Rb = 2$.

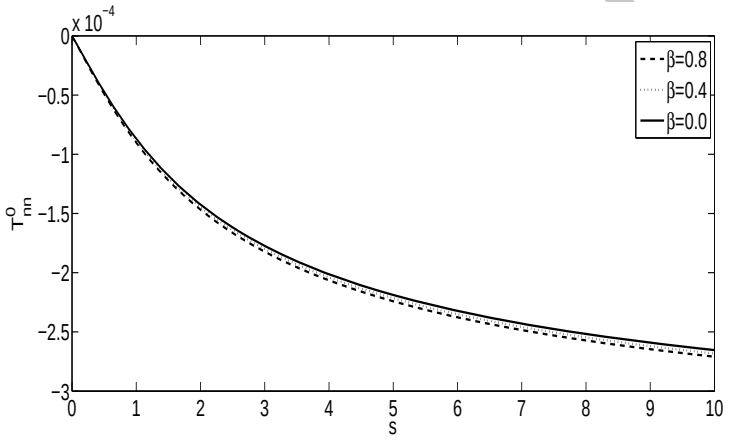

Figure 4: The effect of changing the parameter β of a rotating liquid jet on the extra stress tensor T^0_{nn} along the jet.Here we use $We = 8$, $De = 20$, $\beta = 0.4$, $\alpha_s = 0.2$ and $Rb = 2$.

this parameter leads to an decrease in the radius of the jet which means that the jet becomes thin when the arc-length s is increased. Moreover, on Figs. 3 and 4 we find the relationship between the extra stress tensors, which are T^0_{ss} and T^0_{nn} and the arc-length for different values of the parameter β, and these graphs show that when this parameter increases the extra stress tensors have more effect on the jet.

6. Temporal Instability

In this section we consider small temporal perturbations of the steady state. Since the resulting set of equations must be linearized in terms of the small disturbances we are required to form a simplified expression for the surface tension, which we do through a Taylor expansion as

$$\begin{aligned}\sigma &= (1+\beta log(1-\zeta)) + \sigma^{'}(\zeta)(\Gamma-\zeta) \\ &= (1+\beta log(1-\zeta)) - \frac{\beta}{(1-\zeta)}(\Gamma-\zeta) \\ &= \sigma_e - E\Gamma, \end{aligned} \tag{48}$$

where $\sigma_e = (1+\beta log(1-\zeta)) + \frac{\beta\zeta}{(1-\zeta)}$ is the surface tension of the undisturbed liquid jet and $E = \beta/(1-\zeta)$ is the Gibbs elasticity.
The radius of the jet is of order a, which is comparable to ϵ when $s = O(1)$, when we make perturbations along the jet and so we consider the travelling wave modes of the form

$$(u, R, T_{ss}, T_{nn}, \Gamma) = (u_0, R_0, T^0_{ss}, T^0_{nn}, \Gamma_0) + \delta(\hat{u}, \hat{R}, \hat{T}_{ss}, \hat{T}_{nn}, \hat{\Gamma})\, exp(i\kappa\bar{s} + \omega\bar{t}), \tag{49}$$

where $\bar{s} = s/\epsilon$ is small length scales, $\bar{t} = t/\epsilon$ is small time scales, $k = k(s)$ and $\omega = \omega(s)$ are the wavenumber and frequency of the disturbances and δ is a small constant which is $0 \ll \delta \ll \epsilon^2$ (see Uddin [38]). Whilst the leading order steady state is dependent on the coordinate s the perturbations are functions of the small length scale $\bar{s}$. On this smaller length the steady state is weakly varying and to leading order in $\bar{s}$ is a constant. It is necessary to use the full expression for the mean curvature to prevent instability to waves with zero wavelength which is

$$\frac{1}{We}\left(\frac{1}{R(1+\epsilon^2\, R_s^2)^{\frac{1}{2}}} - \frac{\epsilon^2\, R_{ss}}{(1+\epsilon^2\, R_s^2)^{\frac{3}{2}}}\right).$$

Despite being ad hoc in terms of including higher order terms a number of authors have adopted this approach such as Lee [20] and Eggers [14]. The axial equation of motion becomes

$$\begin{aligned} u_t + u_0 u_{0s} = &-\frac{1}{We}\frac{\partial}{\partial s}\left(\frac{1}{R(1+\epsilon^2\, R_s^2)^{\frac{1}{2}}} - \frac{\epsilon^2\, R_{ss}}{(1+\epsilon^2\, R_s^2)^{\frac{3}{2}}}\right) + \frac{(X+1)X_s + ZZ_s}{Rb^2} \\ &+\frac{3\alpha_s}{Re}\left(u_{0ss} + 2u_{0s}\frac{R_{0s}}{R}\right) + \frac{1}{Re}\Big(\frac{1}{R_0^2}\frac{\partial}{\partial s}\, R_0^2\,(T^0_{ss} - T^0_{nn})\Big), \end{aligned} \tag{50}$$

$$\frac{\partial T^0_{ss}}{\partial t} + u_0 \frac{\partial T^0_{ss}}{\partial s} - 2\frac{\partial u_0}{\partial s} T^0_{ss} = \frac{1}{De}\left(2(1-\alpha_s)\frac{\partial u_0}{\partial s} - T^0_{ss}\right), \quad (51)$$

$$\frac{\partial T^0_{nn}}{\partial t} + u_0 \frac{\partial T^0_{nn}}{\partial s} + \frac{\partial u_0}{\partial s} T^0_{nn} = -\frac{1}{De}\left((1-\alpha_s)\frac{\partial u_0}{\partial s} + T^0_{nn}\right). \quad (52)$$

There is a new scaling for the viscosity ratio which is $\tilde{\alpha_s} = \frac{\alpha_s}{\epsilon}$. Without this new scaling, we cannot bring the viscous term into the equations which derived the dispersion relation. We mentioned earlier, $\alpha_s + \alpha_p = 1$, where α_s and α_p are the solvent viscosity and the polymeric viscosity respectively. After substituting the new scaling, the last equation becomes $\epsilon\tilde{\alpha_s} + \alpha_p = 1$, which means that $\alpha_p \gg \alpha_s$. However, both the solvent viscosity and the polymeric viscosity are very small $\mu_s, \mu_p \ll 1$. Now we obtain the eigenvalue relation at leading order which has the form

$$\omega_r = \frac{-3k^2\tilde{\alpha_s}}{2Re} + \frac{k}{2}\sqrt{\frac{2\sigma_0}{R_0We}\left(1-(kR_0)^2 - \frac{2We}{R_0Re}\right) + \frac{4}{Re}\left(2T^0_{ss} + T^0_{nn} + \frac{3}{De}\right) + \left(\frac{3k\tilde{\alpha_s}}{Re}\right)^2 - \frac{2E\Gamma_0}{WeR_0}}, \quad (53)$$

where ω_r is the growth rate of disturbances and k is the wavenumber, we differentiate the last equation to find the most unstable wavenumber for which ω_r is a maximum (which we refer to as k^*) and from this relation we can find the maximum growth rate

$$k^* = \frac{\sqrt{\frac{R_0GWe}{2} - 2B + (\sigma_0 - \Gamma_0 E)}}{\sqrt{\sqrt{2R_0^3\sigma_0}\left(3\tilde{\alpha_s}\frac{\sqrt{We}}{Re} + \sqrt{2\sigma_0 R_0}\right)}}, \quad (54)$$

where $B = T^0_{ss} - T^0_{nn}$, $G = \frac{4}{\tilde{\alpha_s}Re}\left(2T^0_{ss} + T^0_{nn} + \frac{3}{De}\right)$. For temporal instability, the growth rate ω_r is positive which occurs when $0 < kR_0 < 1$ where $k = k^*$, and R_0 found from the steady state solutions. When $De = 0$ and $T^0_{ss} = T^0_{nn} = 0$ the most unstable wavenumber of a curved viscous jet is

$$k^* = \frac{(\sigma_0 - \Gamma_0 E)^{\frac{1}{2}}}{\sqrt{\sqrt{2R_0^3\sigma_0}\left(3Oh + \sqrt{2\sigma_0 R_0}\right)}}, \quad (55)$$

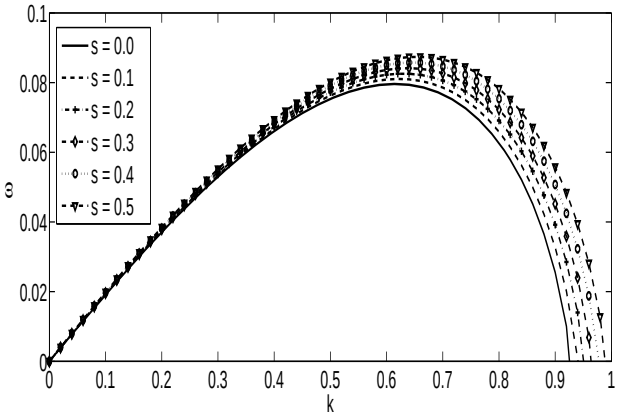

Figure 5: Graph showing the growth rate versus the wavenumber of viscoelastic liquid curved jets with surfactants from a nozzle at $s = 0$ to $s = 0.5$ along the jet. The other parameters here are $We = 10$, $Re = 1000$, $Rb = 2$, $\zeta = 0.2$, $\beta = 0.5$, $De = 20$ and $\tilde{\alpha_s} = 20$.

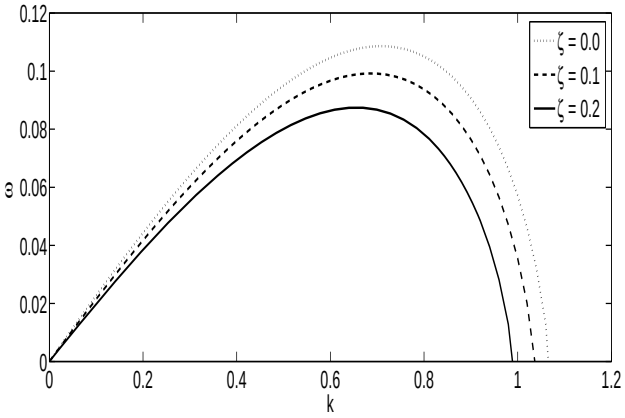

Figure 6: Graph showing the growth rate versus the wavenumber of viscoelastic liquid curved jets with surfactants at the nozzle for different values of the initial surfactant concentration. The other parameters here are $We = 10$, $Re = 1000$, $Rb = 2$, $\zeta = 0.2$, $\beta = 0.5$, $De = 20$ and $\tilde{\alpha_s} = 20$.

where $Oh = \frac{\sqrt{We}}{Re}$ which is the same as for Newtonian liquid jets with surfactant, as found by Uddin [38].

In Fig. 5 we plot the growth rate of a viscoelastic liquid jet with surfactant against the wavenumber for different distances from the nozzle. The

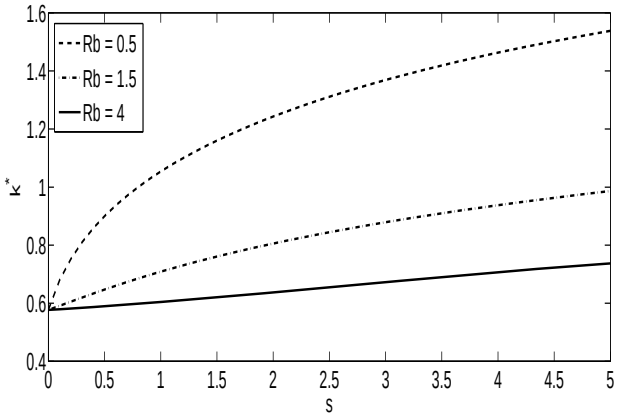

Figure 7: The wavenumber of the most unstable mode k^* versus the arc-length s for different values of the Rossby number. The other parameters here are $We = 15$, $Re = 1000$, $\zeta = 0.5$, $De = 20$, $\tilde{\alpha_s} = 20$ and $\beta = 0.25$.

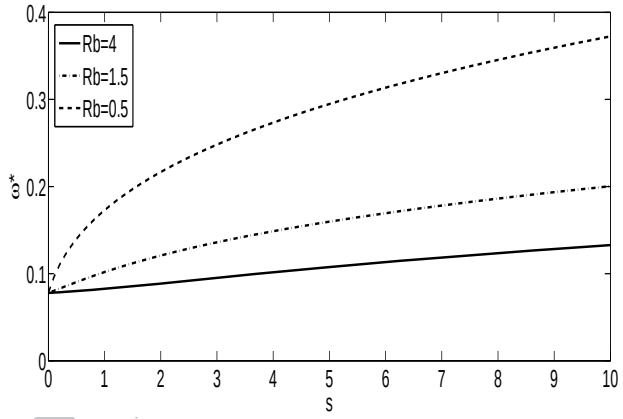

Figure 8: The maximum growth rate ω^* versus the arc-length s for different values of the Rossby number. The other parameters here are $We = 15$, $Re = 1000$, $\zeta = 0.5$, $De = 20$, $\tilde{\alpha_s} = 20$ and $\beta = 0.25$.

presence of a maximum in the plots of the growth rates against wavenumber are indicative of the most unstable wavenumber for this case. The effect of surfactants on viscoelastic liquid curved jets has been examined in Fig. 6 where we can see that when we increase the initial surfactant concentration ζ the growth rate decreases. Consequently this observation agrees with what one would expect given that surfactants lower the surface tension and

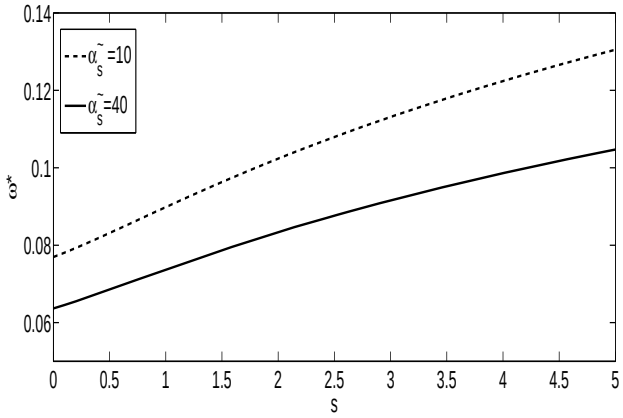

Figure 9: Graph showing the relationship between the growth rate of the most unstable mode ω_r^* and the arc-length s for viscoelastic liquid curved jets with surfactants for two different values of the viscosity ratio $\tilde{\alpha_s}$, where the other parameters here are $We = 15, Re = 1000, \zeta = 0.5, De = 20$ and $\beta = 0.25$.

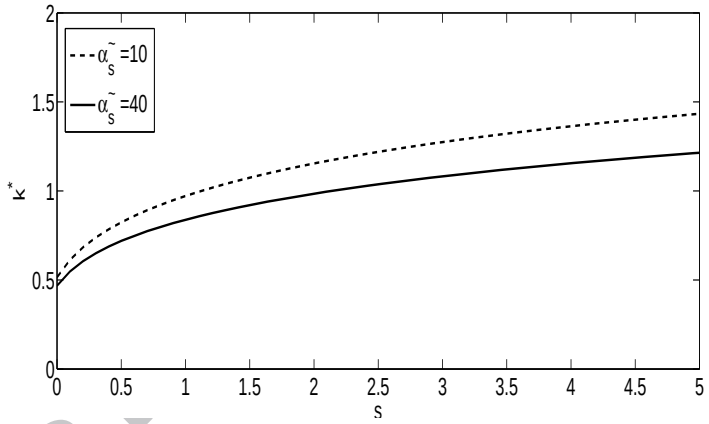

Figure 10: Graph showing the wavenumber of the most unstable mode k^* and the arc-length s of viscoelastic rotating liquid jets with surfactants for two different values of the viscosity ratio $\tilde{\alpha_s}$, where the other parameters here are $We = 15, Re = 1000, \zeta = 0.5, De = 20$ and $\beta = 0.25$.

that the growth of disturbances strongly depends on surface tension. When ζ is increased that leads to a maximum reduction in surface tension (see Chang & Franses [8]). In addition to this, Non-Newtonian liquids formed by accumulation of the broad variety of molecules. It applies above the

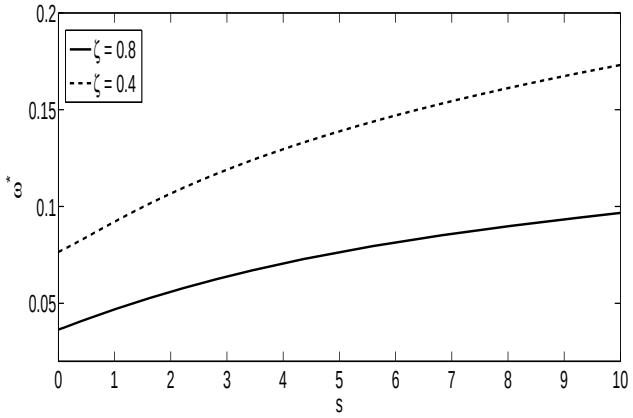

Figure 11: Graph showing the growth rate of the most unstable mode ω^* and the arc-length s of viscoelastic rotating liquid jets with surfactants for two different values of the initial surfactant concentration ζ, where the other parameters here are $We = 15$, $Re = 1000$, $\zeta = 0.5$, $De = 20$ and $\beta = 0.5$.

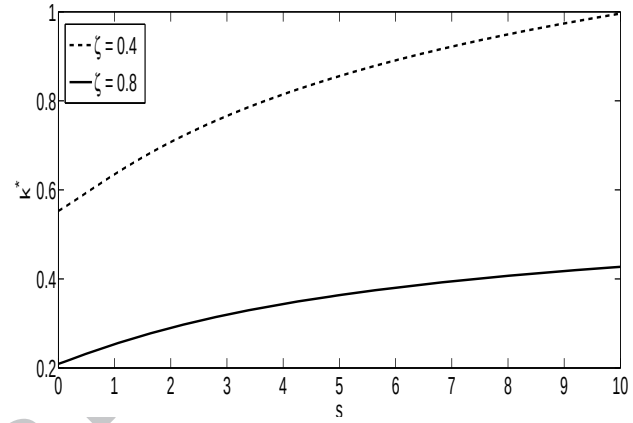

Figure 12: Graph showing the wavenumber of the most unstable mode k^* and the arc-length s of viscoelastic rotating liquid jets with surfactants for two different values of the initial surfactant concentration ζ, where the other parameters here are $We = 15$, $Re = 1000$, $\zeta = 0.5$, $De = 20$ and $\beta = 0.5$.

Critical Micellar Concentration (CMC), where the surfactant molecules can self-assemble to structure aggregates called Micelles. The volume and the nature of the Micelles rely on the composition of the surfactant molecule, on the surfactant absorption and the existence of preservatives like simple or

organic salts. Figs. 7 and 8 show that the wavenumber of the most unstable mode k^* and the maximum growth rate ω^* increase along the jet and that when rotation rates are increased (or equivalently the Rossby number Rb is decreased). Moreover, when we increase the viscosity ratio $\tilde{\alpha_s}$, which in turn leads to a decrease in the polymeric viscosity, the maximum wavenumber and the growth rate are increased which means the liquid is less elastic (see Figs. 9 and 10). In Figs. 11 and 12 we show that when we increase the initial surfactant concentration ζ and the parameter β is fixed the growth rate and the wavenumber of the most unstable mode are decreased which means the liquid jet becomes longer before breakup occurs.

7. Nonlinear Temporal Solutions

Linear instability analysis predicts that liquid jets break-up and produce uniform drop sizes along the axis of the jet of approximately the same wavelength of the initial disturbances. However, in practice a number of smaller satellite droplets appear which are an order of magnitude smaller than the main droplets. This phenomena can only be captured using a nonlinear approach and we therefore use nonlinear temporal analysis to examine the break-up length and the formation of the satellite droplets. In this respects, we replace the leading order pressure term $p_0 = \frac{\sigma}{We}\frac{1}{R_0}$ in the equation (24) with the expression for the full curvature term which contains only R_0 and is not ϕ-dependent, namely

$$p = \frac{\sigma}{We}\left[\frac{1}{R_0(1+\epsilon^2 R_{0s}^2)^{1/2}} - \frac{\epsilon^2 R_{0ss}}{(1+\epsilon^2 R_{0s}^2)^{3/2}}\right]. \tag{56}$$

This is done to correctly simulate the main droplet shapes and has some justification given by Yarin [46]. For simplicity, we denote $A = A(s,t)$, where $A(s,t) = R^2(s,t)$ and $G = \Gamma_0^2$; then we rewrite our equations (50)-(52), (25) and (29) as

$$\frac{\partial u}{\partial t} = -\Big(\frac{u^2}{2}\Big)_s - \frac{1}{We}\frac{\partial}{\partial s}\Big(\sigma\frac{4(2A+(\epsilon A_s)^2 - \epsilon^2 A A_{ss})}{(4A+(\epsilon A_s)^2)^{3/2}}\Big) + \frac{(X+1)X_s + ZZ_s}{Rb^2} + \frac{2\sigma_s}{A^{\frac{1}{2}}We} + \frac{3\alpha_s}{Re}\frac{(Au_s)_s}{A} + \frac{1}{Re}\frac{\Big(A(T_{ss}-T_{nn})\Big)_s}{A}, \tag{57}$$

$$\frac{\partial T_{ss}}{\partial t} = -\frac{\partial}{\partial s}(uT_{ss}) + 3\frac{\partial u}{\partial s}T_{ss} + \frac{1}{De}\Big(2(1-\alpha_s)\frac{\partial u}{\partial s} - T_{ss}\Big), \tag{58}$$

$$\frac{\partial T_{nn}}{\partial t} = -\frac{\partial}{\partial s}(uT_{nn}) - \frac{1}{De}\Big((1-\alpha_s)\frac{\partial u}{\partial s} + T_{nn}\Big), \tag{59}$$

$$\frac{\partial A}{\partial t} = -\frac{\partial}{\partial s}(Au), \tag{60}$$

$$\frac{\partial G}{\partial t} = -\frac{\partial}{\partial s}(Gu). \tag{61}$$

We solve this nonlinear system of equations as we did in section 5 for the steady state by using the initial conditions at $t = 0$ which are $A(s, t = 0) = R_0^2(s),\ u(s, t = 0) = u_0(s), G(s, o) = \Gamma_0^2(s), T_{ss}(s, t = 0) = 0,\ T_{nn}(s, t = 0) = 0$. At the nozzle, we use upstream boundary conditions

$$u(0,t) = 1 + \delta \sin\left(\frac{\kappa t}{\epsilon}\right),\ \Gamma(0,t) = \zeta,\ A(0,t) = 1,$$

where κ is a non-dimensional wavenumber of the perturbation of frequency and δ (of which we used a small size) is the amplitude of the initial non-dimensional velocity disturbance. In the calculation, we have used the value of $\epsilon\,(= \frac{a}{s_0})$ which can be measured from experiments using $\epsilon = 0.01$. This value is the same as found in experiments and industrial problems (see Wong *et al*. [44]).

Profiles have been plotted (Fig. 13) to show the effect of increasing the concentration of initial surfactants on the break-up of viscoelastic liquid curved jets. From this profile we see that when we increase the initial surfactant concentration, the liquid jet becomes longer. We can see from these profiles that there is no beads-on-the string, because this study deals with weakly viscoelastic curved jets. These results also agree with the experiments of Cooper-White *et al*. [10] and Tritaatmadja *et al*. [37] in which show that no beads-on-th string forms for weakly viscoelastic liquid jets. In Fig. 14 we make a comparison between the jet radii against the arc length for the case of liquid jets with and without surfactants. It can readily be observed that adding surfactants on liquid jets delay the break-up of viscoelastic liquid jets and that therefore break-up occurs further down the jet. These results are similar to those found by Uddin [38] for spiralling Newtonian liquid jets with surfactants.

In Fig. 15 we observe that increasing the viscosity ratio α_s makes the liquid jet have a longer break-up length both in the presence of surfactants

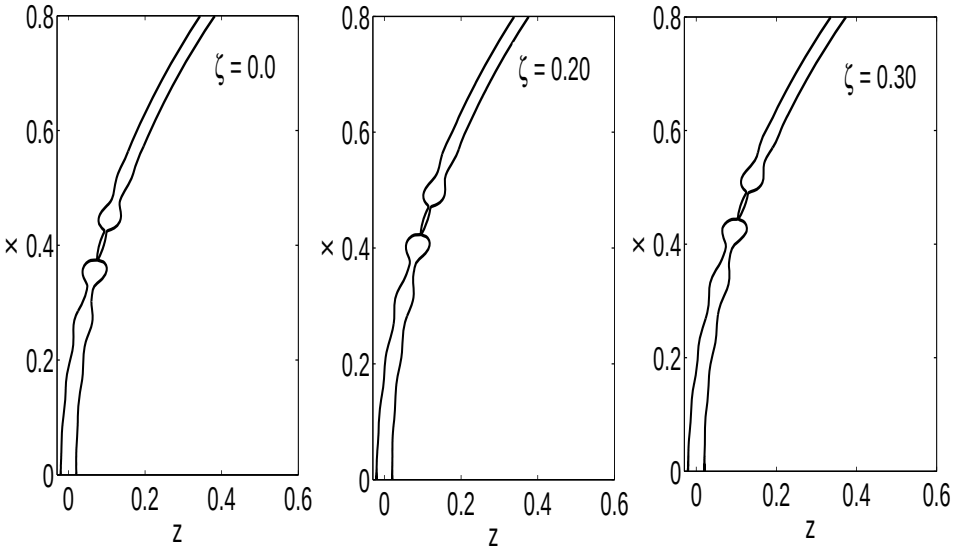

Figure 13: Graph showing viscoelastic liquid curved jets with surfactants by changing the initial surfactant concentration ζ. The parameters here are $Re = 2000$, $We = 10$, $Rb = 2$, $k = 0.7$, $De = 20$, $\delta = 0.01$, $\beta = 0.5$ and $\alpha_s = 0.20$.

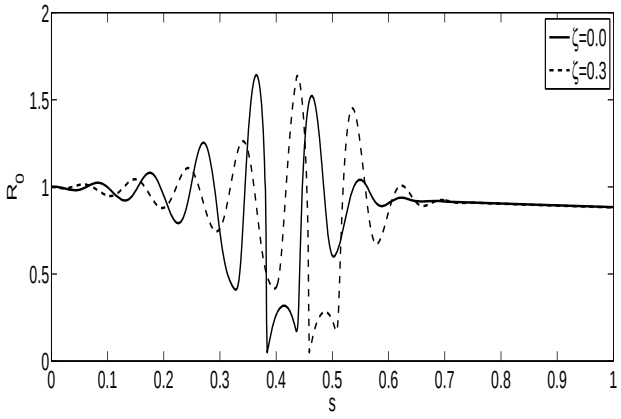

Figure 14: Graph showing the relationship between the radius R_0 and the distance along the jet s with and without surfactants for viscoelastic liquid curved jets. The parameters here are $Re = 2000$, $We = 10$, $Rb = 2$, $k = 0.7$, $De = 20$, $\delta = 0.01$, $\beta = 0.5$ and $\alpha_s = 0.20$.

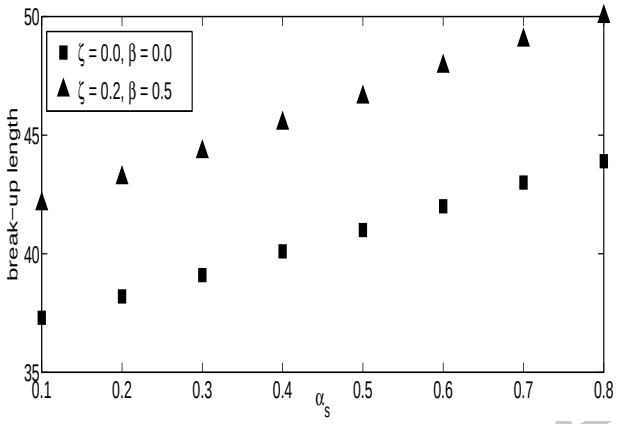

Figure 15: Break-up lengths versus the viscosity ratio α_s of viscoelastic liquid curved jets with and without surfactants. The parameters here are $Re = 2000$, $We = 10$, $Rb = 2$, $De = 20$ and $\delta = 0.01$.

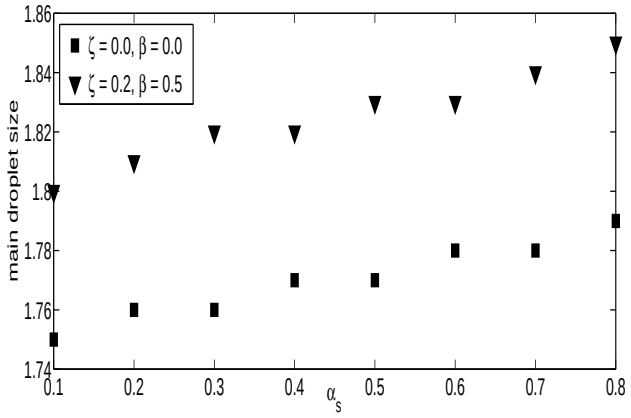

Figure 16: Graph showing the relationship between main droplet sizes and the viscosity ratio α_s with and without the effect of surfactants on viscoelastic liquid curved jets. The parameters here are $Re = 2000, We = 10, Rb = 2, k = 0.8, De = 20$ and $\delta = 0.01$.

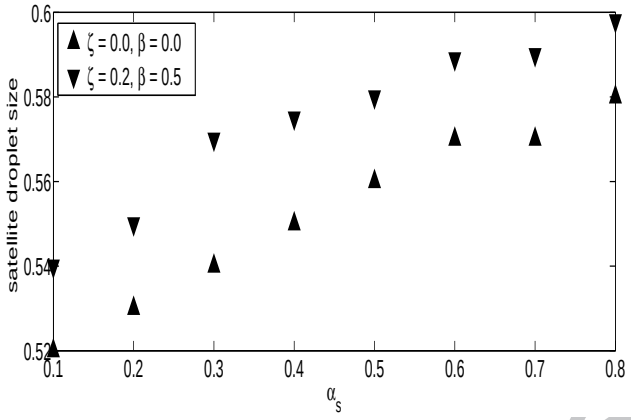

Figure 17: Graph showing the relationship between satellite droplet sizes and the viscosity ratio α_s with and without the effect of surfactants on viscoelastic liquid curved jets. The parameters here are $Re = 2000, We = 10, Rb = 2, k = 0.8, De = 20$ and $\delta = 0.01$.

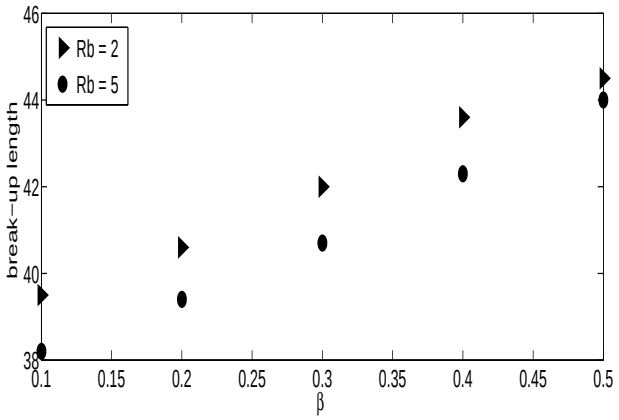

Figure 18: Graph showing the relationship between break-up lengths and the parameter β for two different values of rotation rates Rb with and without the effect of surfactants on viscoelastic liquid curved jets. The parameters here are $Re = 2000$, $We = 10$, $k = 0.8$, $De = 20$, $\zeta = 0.3$, $\delta = 0.01$ and $\alpha_s = 0.20$.

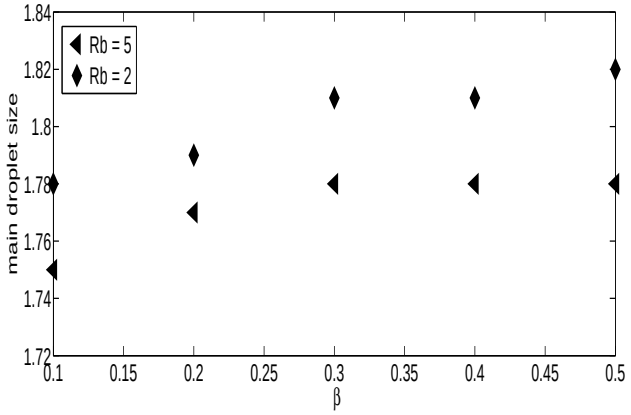

Figure 19: Graph showing the relationship between main droplet sizes versus the parameter β for two different values of rotation rates Rb with and without the effect of surfactants on viscoelastic liquid curved jets. The parameters here are $Re = 2000$, $We = 10$, $k = 0.8$, $De = 20$, $\zeta = 0.3$, $\delta = 0.01$ and $\alpha_s = 0.20$.

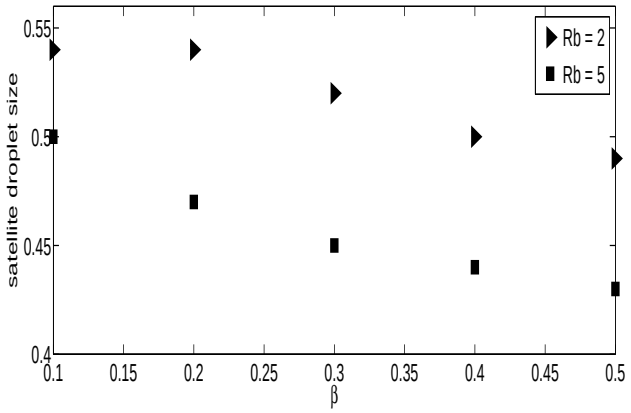

Figure 20: Graph showing the relationship between satellite droplet sizes versus the parameter β for two different values of rotation rates Rb with and without the effect of surfactants on viscoelastic liquid curved jets. The parameters here are $Re = 2000$, $We = 10$, $k = 0.8$, $De = 20$, $\zeta = 0.3$, $\delta = 0.01$ and $\alpha_s = 0.20$.

and without it. Moreover, we plot a graph (Fig. 16) to show main droplet sizes when the viscosity ratio is varied and we see that main droplet sizes are not affected significantly. However, in Fig. 17 it can be noticed that satellite droplet sizes increase when the viscosity ratio is increased.
Now we turn our attention to study the effectiveness of surfactants β. In order to do this, we see in Fig. 18 that increasing the parameter β leads to an increase in the break-up length. In addition, the relationship between main droplet sizes and the parameter β is shown in Fig. 19 and we see that high rotation rates imply an increase the main droplet sizes. In Fig. 20 we show that when the rotation rates are high, satellite droplet sizes decrease with increasing the parameter β. These results are in agreement with Uddin [38].

8. Conclusions

In summary, the Oldroyd-B model has been used to model a viscoelastic liquid curved jet having a layer of surfactants along its free surface. We have used an asymptotic analysis to find the steady state solutions and we have shown that trajectories of viscoelastic rotating liquid jets with surfactants do not affect by the viscosity at leading order. We have also performed the linear instability analysis and examined the growth rate and the most unstable mode for different values of the surfactant concentration. From the linear instability, we have obtained that when we increase the surfactant concentration ζ, the maximum growth rate and the most unstable mode decreases (see Figs. 11 and 12) and this result agreed with Uddin [38]. We have also found that when the viscosity ratio α_s increases, the most unstable mode and its associated the growth rate decreases (see Figs. 9 and 10).
A numerical method based on finite differences has been used to determine break-up lengths, droplet sizes and satellite droplet sizes for viscoelastic liquid curved jets with surfactants. From our results, we can see that break-up lengths and main droplet sizes increase when we add surfactants. Whereas, when we increase the effectiveness of surfactants, as measured by the parameter β, on viscoelastic rotating liquid jets, satellite droplet sizes decrease. This work provides a framework to investigate the effects of variations in fluid rheology and the use of surfactants (both of which are critical in the prilling process) on the size of main and satellite droplets produced. An investigation of the spatio-temporal behaviour of the resulting equations would provide additional information including the occurrence of absolute instability and this work is the object of current work.

9. Acknowledgments

Abdullah Alsharif would like to thank Taif University for their financial support.

10. Appendix A

By using Eq. $(1)_4$, the extra stress tensor equations become

$$\frac{\partial T_{ss}}{\partial t} + \frac{u}{h_s}\frac{\partial T_{ss}}{\partial s} + \frac{v}{\epsilon}\frac{\partial T_{ss}}{\partial n} + \frac{w}{\epsilon n}\frac{\partial T_{ss}}{\partial \phi} - \frac{2}{h_s}\left(\frac{\partial u}{\partial s} + v\,cos\phi - w\sin\phi\right)$$
$$(X_sZ_{ss} - Z_sX_{ss})T_{ss} - \frac{2}{h_s}\left(\frac{\partial v}{\partial s} + \frac{\partial u}{\partial n} - u\cos\phi\,(X_sZ_{ss} - Z_sX_{ss})\right)T_{sn} -$$
$$\frac{2}{h_s}\left(\frac{\partial w}{\partial s} + \frac{1}{n}\frac{\partial u}{\partial \phi} + u\sin\phi\,(X_sZ_{ss} - Z_sX_{ss})\right)T_{s\phi} =$$
$$\frac{1}{De}\left[\frac{2(1-\alpha_s)}{h_s}\left(\frac{\partial u}{\partial s} + (v\cos\phi - w\sin\phi)(X_sZ_{ss} - Z_sX_{ss})\right) - T_{ss}\right], \quad (62)$$

$$\frac{\partial T_{sn}}{\partial t} + \frac{u}{h_s}\frac{\partial T_{sn}}{\partial s} + \frac{v}{\epsilon}\frac{\partial T_{sn}}{\partial n} + \frac{w}{\epsilon n}\frac{\partial T_{sn}}{\partial \phi} - \frac{1}{h_s}\Big(\frac{\partial u}{\partial s} + v\,cos\phi(X_sZ_{ss} - Z_sX_{ss}) -$$
$$w\sin\phi(X_sZ_{ss} - Z_sX_{ss})\Big)T_{sn} - \frac{1}{h_s}\left(\frac{\partial v}{\partial s} + \frac{\partial u}{\partial n} - u\cos\phi\,(X_sZ_{ss} - Z_sX_{ss})\right)T_{nn} -$$
$$\frac{1}{\epsilon}\frac{\partial v}{\partial n}T_{sn} - \frac{1}{h_s}\left(\frac{\partial w}{\partial s} + \frac{1}{n}\frac{\partial u}{\partial \phi} + u\sin\phi\,(X_sZ_{ss} - Z_sX_{ss})\right)T_{n\phi}$$
$$-\Big(\frac{1}{\epsilon}\frac{\partial u}{\partial n} + \frac{1}{h_s}\frac{\partial v}{\partial s} - \frac{u}{h_s}\cos\phi\,(X_sZ_{ss} - Z_sX_{ss})\Big)T_{ss} - \Big(\frac{1}{\epsilon}\frac{\partial w}{\partial n} - \frac{w}{\epsilon n} + \frac{1}{\epsilon n}\frac{\partial v}{\partial \phi}\Big)T_{s\phi}$$
$$= \frac{1}{De}\left[\frac{(1-\alpha_s)}{h_s}\Big(\frac{\partial v}{\partial s} + \frac{h_s}{\epsilon}\frac{\partial u}{\partial n} - u\cos\phi(X_sZ_{ss} - Z_sX_{ss})\Big) - T_{sn}\right], \quad (63)$$

$$\frac{\partial T_{s\phi}}{\partial t} + \frac{u}{h_s}\frac{\partial T_{s\phi}}{\partial s} + \frac{v}{\epsilon}\frac{\partial T_{s\phi}}{\partial n} + \frac{w}{\epsilon n}\frac{\partial T_{s\phi}}{\partial \phi} - \frac{1}{h_s}\Big(\frac{\partial u}{\partial s} + v\,cos\phi(X_sZ_{ss} - Z_sX_{ss}) -$$
$$w\sin\phi(X_sZ_{ss} - Z_sX_{ss})\Big)T_{sn} - \frac{1}{\epsilon}\left(\frac{\partial w}{\partial n} - \frac{w}{n} + \frac{1}{n}\frac{\partial v}{\partial \phi}\right)T_{s\phi}$$
$$-\Big(\frac{\partial u}{\epsilon\partial n} + \frac{1}{h_s}\frac{\partial v}{\partial s} - \frac{u}{h_s}\cos\phi\,(X_sZ_{ss} - Z_sX_{ss})\Big)T_{ss} - \frac{1}{h_s}\Big(\frac{\partial v}{\partial s} + \frac{\partial u}{\epsilon\partial n} -$$

$$u\,\cos\phi(X_sZ_{ss}-Z_sX_{ss})\Big)T_{nn}-\frac{1}{h_s}\Big(\frac{\partial w}{\partial s}+u\,\sin\phi(X_sZ_{ss}-Z_sX_{ss})+\frac{1}{\epsilon n}\frac{\partial u}{\partial\phi}\Big)T_{n\phi}$$
$$=\frac{1}{De}\left[(1-\alpha_s)\left(\frac{1}{\epsilon n}\frac{\partial u}{\partial\phi}+\frac{u}{h_s}\sin\phi(X_sZ_{ss}-Z_sX_{ss})+\frac{1}{h_s}\frac{\partial w}{\partial s}\right)-T_{s\phi}\right], \quad (64)$$

$$\frac{\partial T_{nn}}{\partial t}+\frac{u}{h_s}\frac{\partial T_{nn}}{\partial s}+\frac{v}{\epsilon}\frac{\partial T_{nn}}{\partial n}+\frac{w}{\epsilon n}\frac{\partial T_{nn}}{\partial\phi}$$
$$-2\Big(\frac{1}{\epsilon}\frac{\partial u}{\partial n}+\frac{1}{h_s}\frac{\partial v}{\partial s}-\frac{u}{h_s}\cos\phi\,(X_sZ_{ss}-Z_sX_{ss})\Big)T_{sn}-\frac{2}{\epsilon}\frac{\partial v}{\partial n}T_{nn}$$
$$-\frac{2}{\epsilon}\Big(\frac{\partial w}{\partial n}-\frac{w}{n}+\frac{1}{n}\frac{\partial v}{\partial\phi}\Big)T_{n\phi}=-\frac{1}{De}\left(\frac{2(1-\alpha_s)}{\epsilon}\frac{\partial v}{\partial n}-T_{nn}\right), \quad (65)$$

$$\frac{\partial T_{n\,\phi}}{\partial t}+\frac{u}{h_s}\frac{\partial T_{n\phi}}{\partial s}+\frac{v}{\epsilon}\frac{\partial T_{n\phi}}{\partial n}+\frac{w}{\epsilon n}\frac{\partial T_{n\phi}}{\partial\phi}$$
$$-\Big(\frac{1}{\epsilon}\frac{\partial u}{\partial n}+\frac{1}{h_s}\frac{\partial v}{\partial s}-\frac{u}{h_s}\cos\phi\,(X_sZ_{ss}-Z_sX_{ss})\Big)T_{s\phi}-\frac{1}{\epsilon}\Big(\frac{\partial v}{\partial n}+\frac{1}{n}\frac{\partial w}{\partial\phi}+\frac{v}{n}\Big)T_{n\phi}-$$
$$\frac{1}{\epsilon}\Big(\frac{\partial w}{\partial n}-\frac{1}{n}\frac{\partial v}{\partial\phi}\Big)T_{\phi\phi}-\Big(\frac{1}{\epsilon n}\frac{\partial u}{\partial\phi}+\frac{u}{h_s}\sin\phi\,(X_sZ_{ss}-Z_sX_{ss})+\frac{1}{h_s}\frac{\partial w}{\partial s}\Big)T_{sn}=$$
$$\frac{1}{De}\left[\frac{(1-\alpha_s)}{\epsilon}\Big(\frac{\partial w}{\partial n}-\frac{w}{n}+\frac{1}{n}\frac{\partial v}{\partial\phi}\Big)-T_{n\phi}\right], \quad (66)$$

$$\frac{\partial T_{\phi\phi}}{\partial t}+\frac{u}{h_s}\frac{\partial T_{\phi\phi}}{\partial s}+\frac{v}{\epsilon}\frac{\partial T_{\phi\phi}}{\partial n}+\frac{w}{\epsilon n}\frac{\partial T_{\phi\phi}}{\partial\phi}-\frac{2}{\epsilon n}\left(\frac{\partial v}{\partial\phi}-w+\frac{\partial w}{\partial n}\right)T_{n\phi}$$
$$-2\Big(\frac{1}{\epsilon n}\frac{\partial u}{\partial\phi}+\frac{u}{h_s}\sin\phi\,(X_sZ_{ss}-Z_sX_{ss})+\frac{1}{h_s}\frac{\partial w}{\partial\phi}\Big)T_{s\phi}-\frac{2}{\epsilon n}\left(\frac{\partial w}{\partial\phi}+v\right)T_{\phi\phi}=$$
$$\frac{1}{De}\left[\frac{2(1-\alpha_s)}{\epsilon n}\left(\frac{\partial w}{\partial\phi}+v\right)-T_{\phi\phi}\right]. \quad (67)$$

11. References

References

[1] Ambravaneswaran, B. & Basaran, O. A., Effects of insoluble surfactants on the nonlinear deformation and breakup of stretching liquid bridges. Phys. Fluids, 11 (1999), 997-1015.

[2] Anna, S. L. And Mckinley, G. H., Elasto-capillary thinning and breakup of model elastic liquids. J. Rheol. 45 (2001), 115.

[3] Anshus, B., E., The Effect of Surfactants on the Breakup of Cylinders and Jets, Journal of Colloid and Interface Science, 43 (1973), 113–121.

[4] Ardekani, A. M., Sharma, V., and Mckinley, G. H., Dynamics of bead formation, filament thinning and breakup in weakly viscoelastic jets. J. Fluid Mech. 665 (2010), 46-56

[5] Basaran, O. A., Small-scaled free surface flows with breakup: drop formation and emerging applications. A. I.Ch. E. Journal, 48(9), (2002), 1842-1848.

[6] Bhat, Pradeep P. Appathurai, Santosh, Harris, Michael T. Pasquali, Matteo, McKinley, Gareth H. and Basaran, Osman A., Formation of beads-on-a-string structures during break-up of viscoelastic filaments. Nature Physics, 6 (2010),625-631.

[7] Blyth, M., G., and Pozrikidis, C., Evolution Equations for the surface concentration of an insoluble surfactant; applications to the stability of an elongating thread and a stretched interface, Theoret. Comput. Fluid Dynamics, 17 (2004), 147–164.

[8] Chang, C. H. & Franses, E. I., Adsorption dynamics of surfactants at the air/water interface: a critical review of mathematical models, data and mechanisms. Colloids Surfaces A 100 (1995), 145.

[9] Clasen, C., Eggers, J., Fonlelos, M. A., Li, j., and Mckinley, G. H., The beads-on-string structure of viscoelastic threads. J. Fluid Mech., 556 (2006), 283-308

[10] Cooper-White, J. J., J. E. Fagan, V. Tritaatmadja, D. R. Lester and D. V. Boger, Drop formation dynamics of constant low viscosity, elastic fluids, J. Non-Newtonian Fluid Mech. 106 (2002), 29-59.

[11] Craster, R., V., Matar, O., K., and Papageorgiou, D., T., Pinch off and satellite formation in surfactant covered viscous thread. Phys. Fluids, 14 (2002), 1364–1376.

[12] Decent, S. P., King, A. C. and Wallwork, I. M., Free jets spun from a prilling tower, Journal of Engineering Mathematics, 42 (2002), 265–282.

[13] Decent, S. P., King, A. C., Simmons, M. H., Părău, E. I., Wong, D. C. Y., Wallwork, I. M., Gurney, C., and Uddin, J., The trajectory and stability of a spiralling liquid jet: Part II. Viscous Theory, Appl. Math. Modelling, 33 (12) (2009), 4283–4302.

[14] Eggers, J., Nonlinear dynamics and breakup of free surface flows. Rev. Mod. Physis, 69, (3) (1997), 865–929.

[15] Eggers, J. and Villermaux, E., Physics of liquid jets. Rep. Prog. Phys, 71, 036601(79 pp).

[16] Entov V. W. and Hinch, E. J., Effect of a spectrum of relaxation times on the capillary thinning of a filament of elastic liquid, J. Non-Newtonian Fluid Mech. 72 (1997), 31-53.

[17] Goldin, M., Yerushalmi, J., Pfeffer, R., and Shinner, R., Breakup of a viscoelastic fluid. J. Fluid Mech. 38 (1969), 689–711.

[18] Hansen, S., Peters, G., W., M. and Meijer, H. E. H., The effect of surfactant on the stability of a fluid filament embedded in a viscous fluid, J. Fluid Mech., 382 (1999) 331-349.

[19] Hohman, M. M., Shin, M., Rutledge, G. abd Brenner, M. P., Electrospinning and electrically forced jets. II. Application. Phys. Fluids, 13, (8)(1984), 2221–2236.

[20] Lee, H., C., Drop formation in a liquid jet, IBM J. Res. Dev. 18 (1974), 364.

[21] Mageda, J. J., and Larson, R. G., A transition occurring in ideal elastic liquids during shear flow, J. Non-Newtonian Fluid Mech. 30 (1988), 1–19.

[22] Mckinley, G. H., visco-elasto-capillary thinning and break-up of complex fluids. Rhelogy Reviews, edited by D. M. Binding and K. Walters (British Society of Rhology, Aberystwyth, UK, 2005) pp. 1-48.

[23] Mckinley, G. H. and Tripathi, A. How to extract the Newtonian viscosity from capillary break-up experiments in a filament rheometer. J. Rheol. 44 (2000), 653.

[24] Middleman, S., Modeling Axisymmetric flows; dynamics of films, jets and drops, Academic Press. (1995).

[25] Milliken, W., J., Stone, H., A., and Leal, L. G., The effect of surfactant on the transient motion of Newtonian drops. Phys. Fluids,5 (1993), 69–79.

[26] Milliken, W., J., and Leal., G., The Influence of Surfactant on the Deformation and Breakup of a Viscous Drop : The Effect of Surfactant Solubility. Journal of Colloid and Interface Science, 166 (1994), 275–285.

[27] Papageorgiou, D. T., On the breakup of viscous liquid threads, Phys. Fluids, 7 (1995), 1529.

[28] Părău, E. I., Decent, S. P., King, A. C., Simmons, M. J. H., Wong, D. C. Y., Nonlinear travelling waves on a spiralling liquid jet, Wave Motion, 43 (2006), 599–613.

[29] Părău, E. I., Decent, S. P., Simmons, M. J. H., Wong, D. C. Y. and King, A. C., Nonlinear viscous liquid jets from a rotating orifice, J. Of Eng. Maths. 57 (2007), 159–179.

[30] Rayleigh, W. S., On the instability of jets, Proc. Lond. Math. Soc. 10 (1878), 4.

[31] Renardy, M., A numerical study of the asymptotic evolution and breakup of Newtonian and viscoelastic jets, J. Non-Newtonian Fluid Mech. 59 (1995), 267–282.

[32] Stone, H., A., Bentley, B., J., and Leal, L., G., An experimental study of transient effects in the breakup of viscous drops. J . Fluid Mech. 173 (1986), 131–158.

[33] Press, W., H., Teukolsky, S., A., Vetterling, W., T., and Flannery, B., P., Numerical Recipes in Fortran 77: The art if scientific computing, Cambridge University Press. (2001).

[34] Stone, H., A., and Leal, L., G., The effects of surfactants on drop deformation and breakup. J. Fluid Mech.,220 (1990), 161–186.

[35] Timmermans, M., E., and Lister, J., R., The effect of surfactant on the stability of a liquid thread. J. Fluid Mech.,459 (2002), 289–306.

[36] Tricot, Y. M., Surfactants: static and dynamic surface tension. In Liquid Film Coating (ed. S. F. Kistler & P. M. Schweizer), (1997), pp. 100-136. Chapman & Hall.

[37] Tritaatmadja, V., Mckinley, G. H. and Cooper-White J. J., drop formation and breakup of low viscosity elastic fluids: Effects of molecular weight and concentration, Phys. Fluids, 18 (2006), 043101-1, 043101-18.

[38] Uddin, J., An investigation into methods to control breakup and droplet formation in single and compound liquid jets. PhD thesis, University of Birmingham. (2007).

[39] Uddin, J., Decent, S. P., and Simmons. M. J. H. The instability of shear thinning and shear thickening spiralling liquid jets: Linear theory. ASME J. of Fluids Eng., 128 (2006), 968-975.

[40] Wallwork, I. M., The trajectory and stability of a spiralling liquid jet, Ph.D. Thesis, University of Birmingham, Birmingham. (2002a).

[41] Wallwork, I. M., Decent, S.P., King, A. C. and Schulkes, R. M. S., The trajectory and stability of a spiralling liquid jet. Part 1, Inviscid Theory, J. Fluid Mech., 459 (2002b), 43–65.

[42] Weber, C., Zum Zerfall eines Flussigkeitsstrahles. Z. Angew. Math. Mech, 11 (1931), 136–154.

[43] Whitaker, S., Studies of the Drop-Weight Method for Surfactant Solutions III. Journal of Colloid and Interface Science, 51 (1976), 231–248.

[44] Wong, D. C. Y., Simmons, M. J. H., Decent, S. P., Parau, E. I. and King, A. C., Break-up dynamics and drop sizes distributions created from spiralling liquid jets, International Journal of Multiphase Flow. 30 (5), (2004), 499–520.

[45] Xue, Z., Corvalan C. M., Dravid v. and Sojka, P. E., Breakup of shear-thinning liquid jets with surfactants, Chemical Engineering Science, 63 (2008), 1842 1849.

[46] Yarin, A. L., Free Liquid Jets and Films: Hydrodynamics and Rheology. Longmore, New York (1993).

[47] Zhang, X. and Basaran, O. A., An experimental study of dynamics of drop formation. Phys. Fluids, 7 (1995), 1184.

[48] Zhang, Y. L., Matar, O. K., Craster, R. V., Surfactant spreading on a thin weakly viscoelastic film. J. Non-Newtonian Fluid Mech., 105 (2002), 53–78.

[49] Zhang, X., Padgett, R. S. & Basaran, O. A., Nonlinear deformation and breakup of stretching liquid bridges. J. Fluid Mech. 329 (1996), 207.

[50] Yildirim, O. E. and Basaran, O. A., Deformation and breakup of stretching bridges of Newtonian and shear-thinning liquids: comparison of one-and two-dimensional models. Chemical Engineering Science, 56 (1), (2001), 211-233.

Highlights

1- We model viscoelastic rotating liquid jets with surfactants
2- Increasing surfactants leads to different growth rates
3- Altering rotation rates leads to differences in growth rates
4- Steady state solutions are affected by surfactants and rotation

Abdullah Alsharif